

1 **Title**

2

3 **Rapid surveillance platforms for key SARS-CoV-2 mutations in**

4 **Denmark**

5

6 **Authors**

7 Katja Spiess<sup>1,5#</sup>, Vithiagarun Gunalan<sup>1,5</sup>, Ellinor Marving<sup>1</sup>, Sofie Holdflod Nielsen<sup>2</sup>,  
8 Michelle G. P. Jørgensen<sup>2</sup>, Anna S. Fomsgaard<sup>1</sup>, Line Nielsen<sup>2</sup>, Alonzo Alfaro-  
9 Núñez<sup>1</sup>, Søren M. Karst<sup>1</sup>, The Danish COVID-19 Genome Consortium (DCGC)<sup>4</sup>,  
10 Shila Mortensen<sup>1</sup>, Morten Rasmussen<sup>1</sup>, Ria Lassaunière<sup>1</sup>, Maiken Worsøe  
11 Rosenstjerne<sup>3</sup>, Charlotta Polacek<sup>1</sup>, Jannik Fonager<sup>1</sup>, Arieh S. Cohen<sup>2</sup>, Claus Nielsen<sup>1</sup>,  
12 Anders Fomsgaard<sup>1</sup>

13

14 **Affiliation**

15 <sup>1</sup> Department of Virus and Microbiological Special Diagnostics, Statens Serum  
16 Institut, Artillerivej 5, 2300 Copenhagen S, Denmark

17 <sup>2</sup> Test Center Danmark, Statens Serum Institut, Artillerivej 5, 2300 Copenhagen S,  
18 Denmark

19 <sup>3</sup> Qlife Aps. Symbion, Fruebjergvej 3, 2100 Copenhagen Ø, Denmark

20 <sup>4</sup> <https://www.covid19genomics.dk/about>

21 <sup>5</sup> These authors contributed equally

22 #Corresponding author: Katja Spiess, [ktsp@ssi.dk](mailto:ktsp@ssi.dk)

23

24

25 **Abstract**

26

27 Multiple mutations in SARS-CoV-2 variants of concern (VOCs) may increase,  
28 transmission, disease severity, immune evasion and facilitate zoonotic or  
29 anthroprozoonotic infections. Four such mutations, ΔH69/V70, L452R, E484K and  
30 N501Y, occur in the SARS-CoV-2 spike glycoprotein in combinations that allow  
31 detection of the most important VOCs. Here we present two flexible RT-qPCR  
32 platforms for small- and large-scale screening to detect these mutations, and schemes  
33 for adapting the platforms for future mutations. The large-scale RT-qPCR platform,  
34 was validated by pair-wise matching of RT-qPCR results with WGS consensus  
35 genomes, showing high specificity and sensitivity. Detection of mutations using this  
36 platform served as an important interventive measure for the Danish public health  
37 system to delay the emergence of VOCs and to gain time for vaccine administration.  
38 Both platforms are valuable tools for WGS-lean laboratories, as well for  
39 complementing WGS to support rapid control of local transmission chains worldwide.

40

41

42 **Keywords**

43 Pandemic, SARS-CoV-2, key mutations, variant of concern, variant of interest, RT-  
44 qPCR, large scale screening, whole genome sequencing, national surveillance  
45 program

46

NOTE: This preprint reports new research that has not been certified by peer review and should not be used to guide clinical practice.

47

## 48 Introduction

49

50 The global SARS-CoV-2 pandemic, which raised with the identification of this novel  
51 coronavirus in late 2019, has seen the emergence of several variants, each with a  
52 distinct set of mutations<sup>1</sup>. Early detection of new SARS-CoV-2 mutations and  
53 associated measures to decrease the risk of spread are important to control local  
54 outbreaks of SARS-CoV-2 variants, especially those which have been designated  
55 Variants of Concern (VOCs)<sup>2,3</sup>. The latter are defined by increased transmissibility,  
56 severity of infections and resistance to immunity<sup>4-8</sup>. VOCs include the Alpha  
57 (B.1.1.7) and (B.1.1.7 + E484K), Beta (B.1.351), Gamma (P1) and Delta (B.1.617.2)  
58 variants (**Fig.1A-C/Tab. 1**).

59

60

**Table 1/Overview of SARS-CoV-2 variants, occurrence and evidence of impact**

Variant of concern	Variant	First Observed/ Country	Impact on Transmissibility	Impact on Severity	Impact on Immunity
Alpha*	B.1.117	September 2020/ United Kingdom	Yes <sup>5</sup>	Yes <sup>8</sup>	No
Beta	B.1.351	September 2020/South Africa	Yes <sup>9</sup>	Yes <sup>8,10</sup>	Yes <sup>9,11</sup>
Gamma	P.1	December 2020/ Brazil	Yes <sup>12</sup>	Yes <sup>8</sup>	Yes <sup>7</sup>
Delta	B.1.617.2	December 2020/India	Yes <sup>13</sup>	Yes <sup>6,13,14</sup>	Yes <sup>6,14,15</sup>

61

62

63

\* former variant of concern, now classified as de-escalated variant/ adapted from<sup>5</sup>

64

65

66

67

68

69

70

71

72

73

74

75

76

77

78

79

80

81

82

83

84

85

86

87

88

In all these VOCs, combinations of key mutations are present in *S*: N501Y in the variants Alpha (B.1.1.7), Beta (B.1.351) and Gamma (P.1); E484K in the variants Beta (B.1.351) and Gamma (P.1) and within the emerging Alpha B.1.1.7 variant<sup>16</sup>; L452R in the Delta (B.1.617.2) variant and  $\Delta$ H69/V70 in the variants Alpha (B.1.1.7) and B.1.1.298.

The N501Y mutation occurs in the receptor-binding interface and confers a substantial increase in the binding affinity of the *S* for the human angiotensin-converting enzyme 2 (hACE2) protein<sup>17</sup>. HACE2 interaction with the *S* is essential for virus entry and infection of the cells<sup>18</sup>. The E484K mutation has been identified as an immunodominant spike protein residue, facilitating escape from several monoclonal antibodies, as well as antibodies in convalescent plasma<sup>19-21</sup>. Altered immune recognition has also been described for the L452R mutation<sup>21-23</sup>. The key mutation  $\Delta$ H69/V70, a two amino acid deletion, has appeared in multiple SARS-CoV-2 variants at different geographical locations across Europe. In Denmark,  $\Delta$ H69/V70 was detected in local outbreaks in mink farms in Northern Jutland<sup>24,25</sup>. The spread of this deletion in combination with additional mutations (notably Y453F) resulted in the SARS-CoV-2 mink variants B.1.1.298, which transmitted both ways between humans and mink; also giving rise to the early “cluster 5” variant<sup>24,26</sup>.

The identification of these variants and the mutations that form their signature are largely dependent on Whole Genome Sequencing (WGS) of SARS-CoV-2 from infected individuals. In addition, WGS of SARS-CoV-2 also elucidates sets of novel mutations potentially linked to changes in viral properties or associated with vaccine breakthrough. However, the utility of WGS in a pandemic such as this also carries with it a significant cost in the form of reagents, equipment as well as turnaround time

89 – the average time from sample to genome being ~1-7 days depending on the scale of  
90 sequencing performed. This has led to the development of alternatives to WGS such  
91 as SARSeq, which is based on sequencing of the ectodomain of the SARS-CoV-2  
92 spike protein<sup>27</sup> or sequencing of the whole S gene using Sanger sequencing<sup>28</sup>.  
93 While such approaches yield cost and reagent savings, the turnaround time,  
94 preparation effort for these and cost are still higher compared to RT-qPCR detection  
95 platforms. In addition, qPCR technology is inarguably one of the cornerstones of  
96 modern infectious disease diagnostics, thus expertise and equipment is readily  
97 available and is not hindered by technical issues that might present themselves with  
98 newer technologies, which could potentially delay the implementation of such  
99 screening approaches. In order to detect SARS-CoV-2 mutations in near real-time  
100 after sample acquisition and to allow for implementation at different scales (both  
101 small and large), we developed fast, robust and flexible RT-qPCRs platforms using  
102 state-of-the-art modified detection probes. Small-scale screening entails the  
103 simultaneous detection of three key mutations in a multiplexed RT-qPCR, where sets  
104 of variant-specific mutations can be replaced by a single signature mutation of  
105 concern such as for the Delta (B.1.617.2) variant with the L452R mutation. The large-  
106 scale screening strategy entails the detection of four key mutations by a combination  
107 of multiplexed and single RT-qPCRs running in parallel in a 384-well format.  
108 Validation of the large-scale implementation of this RT-qPCR platform was  
109 performed for 9572 positive samples collected between 6<sup>th</sup> June 2021 and 11<sup>th</sup> July  
110 2021 as part of the national surveillance program in Denmark using paired WGS  
111 consensus genomes derived from SARS-CoV-2 positive samples. From here, the  
112 specificity, sensitivity, Positive Predictive Value (PPV) and Negative Predictive  
113 Value (NPV) were determined for the large-scale RT-qPCR platform. The RT-qPCR  
114 platforms for both small- and large-scale screening are designed as flexible detection  
115 systems, where new mutations of concern can be included, thereby following the  
116 course of the pandemic with minimal lag time.

117  
118

## 119 **RESULTS**

120

### 121 **SMALL SCALE SCREENING OF SARS-COV-2 VARIANTS OF CONCERN**

122

123 For laboratories with small amounts of positive SARS-CoV-2 samples or without the  
124 capacity to screen on a large scale for SARS-CoV-2 variants we developed a  
125 multiplexed RT-qPCR (**v.1**) that can detect three key mutations ( $\Delta$ H69/V70, E484K  
126 and N501Y) simultaneously (**Fig. 2A**). As proof of concept to determine if a key  
127 mutation can be replaced by another, we replaced the  $\Delta$ H69/V70 with the L452R  
128 mutation present in the delta variant (B.1.617.2) in the multiplex RT-qPCR (**v.2**) (**Fig.**  
129 **2B**).

130

#### 131 **Multiplexed RT-qPCR v.1**

132

133 As a first step in the multiplexed RT-qPCR v.1 we developed a primer/probe pair  
134 detecting the  $\Delta$ H69/V70 and WT sequence, respectively (**Fig. 2C-D**). The limit of  
135 detection of the  $\Delta$ H69/V70 RT-qPCR was 5 copies/ $\mu$ l for the  $\Delta$ H69/V70 performing a  
136 dilution series with a PCR standard TWIST control (Alpha B.1.1.7) (**Fig. 3E/ Suppl.**  
137 **Tab.2**). PCR-positive SARS-CoV-2 patient samples with paired consensus genomes  
138 from WGS were included into the  $\Delta$ H69/V70 RT-qPCR. The  $\Delta$ H69/V70 or WT

139 nucleotide sequence was detected independent of the concentration of the SARS-  
140 CoV-2 sample (amount of SARS-CoV-2 RNA included per sample into the PCR)  
141 (**Fig. 2F**) and could be detected in samples of the Alpha B.1.1.7, B.1.258 and  
142 B.1.1.298 variants, where this key mutation is present (**Suppl. Fig. 1A-C**). The  
143  $\Delta$ H69/V70 RT-qPCR correctly detected the  $\Delta$ H69/V70 in SARS-CoV-2 positive  
144 samples and did not amplify samples positive for respiratory tract viruses other than  
145 SARS-CoV-2 (10/10 samples) (**Suppl. Tab. 3**). After successful validation, this RT-  
146 qPCR was incorporated as a part of the national surveillance program in Denmark  
147 driven by TestCenter Denmark, as a large-scale screen for SARS-CoV-2 variants  
148 harbouring  $\Delta$ H69/V70 (starting on December 18, 2021). By mid-February 2021 the  
149 Alpha B.1.1.7 variant was the most prominent variant in Denmark (**Fig. 2G**) and at  
150 the end of March, about 80% of all SARS-CoV-2 patient samples were tested positive  
151 for the  $\Delta$ H69/V70 deletion (**Fig. 2I**), which was confirmed by WGS (**Fig. 2H, Suppl.**  
152 **Fig. 1D**). Therefore, it was investigated if the  $\Delta$ H69/V70 RT-qPCR could be  
153 multiplexed, which would then allow for the incorporation of further mutations  
154 present in other Variants of Concern. While the Alpha (B.1.1.7) variant was the most  
155 dominant variant in that time period, Beta (B.1.351) and Gamma (P.1) were still  
156 circulating in Denmark (**Suppl. Fig 1 D**). As a first step, the  $\Delta$ H69/V70 RT-qPCR ran  
157 together with the diagnostic SARS-CoV-2 E-Sarbeco PCR (E-gene)<sup>29</sup>. The sensitivity  
158 of the  $\Delta$ H69/V70 RT-qPCR was found not to be reduced when multiplexed with the  
159 E-Sarbeco RT-qPCR (**Suppl. Fig. 1E**). In conclusion, the  $\Delta$ H69/V70 RT-qPCR was  
160 determined to be sensitive and specific for the detection of the  $\Delta$ H69/70 as well as  
161 insensitive to multiplexing. To detect further key-mutations present in SARS-VOCs  
162 (Alpha/Beta/Gamma/Delta) and other variants of interest, we developed primers and  
163 probes to detect the L452R, E484K and N501Y mutations. Compared to the  
164  $\Delta$ H69/V70 deletion where the probe targets a stretch of a deletion of six nucleotides,  
165 the probes for the three key mutations listed above differ only by one nucleotide  
166 substitution within the *S*. Therefore, we increased their binding affinity to the  
167 mutations or the WT sequence by modifying the probes as black whole quencher  
168 plus- (BHQplus), locked nucleic acid- (LNA) or minor groove binding (MGB)  
169 conjugated probes. For the different RT-qPCRs, we tested for each mutations all  
170 primer and probe combinations, with all three probe modifications. For the N501Y  
171 mutation e.g., the MGB-conjugated probes for the N501Y mutation in the RT-qPCR  
172 were observed to be superior to locked nucleic acid (LNA) - conjugated probes, where  
173 a specific signal was detected for either the mutation or WT sequence. In contrast, the  
174 LNA probes in the N501Y RT-qPCR detected the right mutations present in the  
175 variants, but additional allelic discrimination analysis was needed to discriminate  
176 between the intensity of the signal for the mutation or the WT probe at a Ct of 45  
177 (**Suppl. Fig. 2A-D**).

178 For the L452R mutation, BHQ plus conjugated probes were found to be absolutely  
179 specific compared to the LNA- and MGB conjugated probes (**Fig. 3A-B**). The limit of  
180 detection for L452R was determined by a dilution series of a patient sample with  
181 known sequence information for the delta variant (B.1.617.2) and tested in parallel in  
182 the L452R RT-qPCR and the E-Sarbeco RT-qPCR (**Fig. 3C**). The L452R RT-qPCR  
183 was about 2-fold less sensitive than the E-Sarbeco RT-qPCR (**Fig. 3C**).

184 The best results for the E484K mutation were gained using MGB - conjugated probes  
185 that were refined to generate a signal specific to mutation or WT nucleotide,  
186 respectively (**Fig. 3D-E, G-H**). The limit of detection for the E484K RT PCR was  
187 found to be 52 and 5 copies/ $\mu$ l respectively, performing a dilution series with the  
188 TWIST control Beta B.1.351 and Gamma P.1 (**Fig. 3F, I, Suppl. Tab.1**).

189

190 As a signal detected was specific either for the key mutations or the WT sequence, it  
191 was possible to only include the probes detecting the key mutations (L452R, E484K  
192 and N501Y) or the  $\Delta$ H69/V70 into the multiplexed RT-qPCRs **v.1** and **v.2** (**Fig. 3J-**  
193 **O**). The probe for the  $\Delta$ H69/70 was further modified as a Zen-conjugated probe in the  
194 multiplexed RT-qPCR v.1 to increase the signal intensity for this probe competing  
195 with the MGB-conjugating probes for E484K and N501Y mutations. Testing SARS-  
196 CoV-2 positive patient samples with known whole genome sequence information in  
197 the multiplexed RT-qPCR (**v.1**), the key mutations  $\Delta$ H69/V70, E484K and N501Y  
198 present in the Alpha (B.1.17), Beta (B.1.351), B.1.5125 and P.2 were detected  
199 simultaneously if present in all patient samples (23/23) (**Fig. 3J-L**) (**Suppl. Tab 4**).  
200 The limit of detection for the different mutations was moderately reduced to around  
201 50 copies/ $\mu$ l for the different mutations in the multiplexed RT-qPCR v.1 (**Suppl.**  
202 **Tab.6**). To determine the specificity of the RT-qPCR v.1 we tested samples  
203 containing respiratory tract viruses other than SARS-CoV-2. Five positive signals  
204 could be detected for samples of respiratory tract viruses, but with a CT higher than  
205 38 in the multiplexed **RT-qPCR v.1** (**Suppl. Tab. 5**). Repeating the experiments  
206 twice with the same samples in **RT-qPCR v.1** resulted in a negative result (**Suppl.**  
207 **Tab.5**). As the limit of detection for the multiplex **RT-qPCR v.1** was at a CT of 37  
208 for the N501Y mutation, positive Ct values > 38 should be considered as negative  
209 (**Suppl. Tab. 6**).

210

### 211 **Multiplexed RT-qPCR v.2**

212

213 As proof of concept and to investigate the robustness of the multiplexed RT-PCR we  
214 investigated if the  $\Delta$ H69/V70 could be replaced by the L452R mutation, present in the  
215 delta variant (B.1.617.2) in the multiplexed **RT-qPCR v.2**. As it is recommended to  
216 limit the number of MGB-conjugated probes in a multiplex RT-qPCR, we combined  
217 the two MGB-conjugated probes for the E484K and N501Y mutations with a BHQ-  
218 plus-conjugated probe for the L452R mutation. With this approach the three key  
219 mutations L452R, E484K and N501Y could be simultaneously detected in 31/31  
220 samples with known sequence information for the alpha (B.1.1.7), beta (B.1.351) and  
221 zeta (P.2) variants in the multiplexed **RT-qPCR v.2** (**Suppl. Tab.3**).

222

223 The multiplexed small-scale RT-qPCR platform offers a flexible and fast detection  
224 system to rapidly identify key mutations present in SARS-CoV-2 VOCs and  
225 mutations of interest. Notably, new key mutations can be accommodated by  
226 exchanging one of the existing sets. This forms the basis of a flexible detection  
227 platform where three key mutations can be detected in parallel in the multiplexed RT-  
228 qPCRs for small-scale screening.

229

230

### 231 **LARGE SCALE SCREENING OF THE VARIANT RT-qPCR AS PART OF** 232 **THE NATIONAL SURVEILLANCE PROGRAM IN DENMARK**

233

234 The same primer and probes designed for the four key mutations ( $\Delta$ H69/V70, L452R,  
235 E484K and N501Y) included into the multiplexed RT-qPCR for small-scale screening  
236 were further validated for large-scale screening, implemented to support the national  
237 surveillance program in Denmark in addition to WGS, supporting the public health  
238 system to delay the emergence of VOC. Large-scale screening consisted of RT-

239 qPCRs running in parallel on a 384-well plate allowing for parallel detection of the  
240 four key mutations. The two key mutations,  $\Delta$ H69/V70 and N501Y run as  
241 multiplexed RT-qPCR in large scale, were detected in 17/17 (100 %) of patient  
242 samples with known sequence for the Alpha (B.1.1.7) and Beta (B.1.351) variants  
243 (**Suppl. Tab. 7**). The L452R and E484K mutations were correctly detected in single  
244 RT-qPCR reactions in 18/18 (100%) and 31/31 (100 %) patient samples respectively,  
245 with known sequence information for the Alpha (B.1.1.7), Beta (B.1.351), Delta  
246 (B.1.617.2), Zeta (P.2) or B.1.525 variants (**Suppl. Tab. 8-9**). The  
247  $\Delta$ H69/V70/N501Y, L452R and E484K RT-qPCRs for large-scale screening were  
248 specific, as these did not yield a positive signal in samples positive for common  
249 respiratory tract viruses other than SARS-CoV-2 (**Suppl. Tab.2**). Based on these  
250 results, the RT-qPCRs were implemented into the large-scale screening at TestCenter  
251 Denmark, where the sensitivity and specificity were tested in comparison to WGS  
252 data (**Fig. 4A-C**).

253 To validate the RT-qPCR implemented as large-scale screening, results from 9572  
254 positive samples were tested both in the RT-qPCR and by WGS over a five-week  
255 period from the 7<sup>th</sup> of June 2021 to the 11<sup>th</sup> of July 2021 were compared. This period  
256 was selected due to the presence of all four key mutations of interest in genomes  
257 sequenced as part of this national surveillance strategy. It is also during this period the  
258 dominant B.1.1.7 (Alpha) SARS-CoV-2 variant<sup>30</sup> was seen to be replaced by the more  
259 transmissible<sup>31</sup> B.1.617.2 (Delta) variant in Denmark. This then allowed for a rigorous  
260 test of the RT-qPCR strategy due to the presence and absence of these key mutations  
261 amongst these multiple variants (**Fig. 1A-B**). A daily range of 150 to 671 samples  
262 were analysed by multiplex RT-qPCR during this period and results were  
263 characterised as either positive (POS) or negative (NEG) for a given key mutation  
264 (**Fig. 4C**). It was observed that there was a small number of inconclusive results  
265 amongst the E484K RT-qPCRs, as well as a more noticeable number of inconclusive  
266 results in the N501Y RT-qPCR which could be attributed to probe manufacturing  
267 issues beyond our control – replacement of the probes resulted in a significant  
268 reduction in the number of inconclusive results from this reaction (**Fig. 4C**/lower left  
269 panel), Jul 10<sup>th</sup> to Jul 11<sup>th</sup>, 2021). This probe was found to be more sensitive to the  
270 concentration of the samples, thus samples with high CT values in the initial E-  
271 Sarbeco based analysis had a tendency to yield inconclusive results. Thus, the N501Y  
272 RT-qPCR was more sensitive to minor variations in batch quality. In order to validate  
273 all RT-qPCR results and determine the specificity and sensitivity of these  
274 primer/probe combinations, WGS consensus genomes from the same samples were  
275 used as a reference standard.

276  
277 WGS was performed on all positive samples during the study period using the  
278 ARCTIC Network's PCR scheme v3 (see Materials and Methods) and the aligned *S*  
279 gene sequences from the resulting consensus genomes were used to validate the  
280 results of each of the three RT-qPCR reactions, by comparison of translated codons to  
281 RT-qPCR results at each position encoding the four key mutations of interest in this  
282 study. Validation was performed on samples where both a valid RT-qPCR result and a  
283 consensus genome sequence was obtained, a number which differed for each of the  
284 four key mutations for various technical reasons anticipated at this scale (see above).  
285 The validation results (**Fig. 5**) showed good agreement between amino acids  
286 translated from WGS and RT-qPCR results for E484K, N501Y and L452R (**Fig. 5A-**  
287 **C**). The determination of concordance proved less straightforward for  $\Delta$ H69/V70 due  
288 to the alignment of reads around the deletion prior to consensus generation, resulting

289 in a significant discordant fraction between the deletion and negative RT-qPCR  
290 results (**Fig. 5D**). It was also observed amongst the consensus genomes used in this  
291 validation that amino acid 452 in the spike protein was more mutable than the other  
292 positions which form this set of key mutations, with L, R, M and Q observed at this  
293 position depending on the lineage (Q484 was not observed in genomes during the  
294 selected period but has been recorded in global surveillance data).

295  
296 In order to meaningfully compare and describe the relative performance of the RT-  
297 qPCR strategy from the results of the large-scale screen, as well as to determine the  
298 true-positive or true-negative rate of these combinations of primers and probes, the  
299 specificity and sensitivity of each primer/probe combination was determined using  
300 established methods used to characterise diagnostic testing<sup>32</sup>. Using the validation of  
301 the RT-qPCR with WGS as a reference standard, specificities and sensitivities were  
302 calculated for all primers and probes for the four key mutations, and it was observed  
303 that all four RT-qPCRs were highly specific (>99.9%), and three out of four assays  
304 were highly sensitive (>99.9%) (**Fig. 5 A-D**). The sensitivity of the probe for  
305 detection of  $\Delta$ H69/V70 was observed to be reduced (79.28%) due to a significant  
306 number of deletions in WGS, which were assayed to be negative by RT-qPCR;  
307 however, given the challenge of read alignments around genomic regions containing  
308 insertions or deletions, this was postulated to be largely due to the determination of  
309 the deletion in WGS consensus genomes. In addition to the specificity and sensitivity  
310 of the primer/probe combinations, the Positive Predictive Value (PPV) and Negative  
311 Predictive Value (NPV) of these combinations was also determined, which indicates  
312 the ability of a diagnostic assay or test to accurately detect a condition or in this case,  
313 mutation<sup>32</sup>. The determination of PPV and NPV takes into account the specificity and  
314 sensitivity of the primer/probe combinations as well as the prevalence of the four key  
315 mutations amongst the sequenced SARS-CoV-2 genomes during the study period:  
316 It was determined that all four primer/probe combinations had a PPV of at least 97 %,  
317 and a NPV of 99.9 % for three out of four of these, with the  $\Delta$ H69/V70 assay having a  
318 NPV of 75.43 % (**Fig. 5 A-D**). From the results of the large-scale screening, it can be  
319 seen therefore that the specificity and sensitivity as well as the PPV and NPV all point  
320 towards the viability of this RT-qPCR strategy in a large-scale diagnostic setting.

321  
322  
323

**Tab 3 Positive and Negative Predictive Values for all 4 RT-qPCR assays during period of large-scale screen (7<sup>th</sup> June 2021 to 11<sup>th</sup> July 2021).**

Mutation	Prevalence (%) (No. of samples)	PPV (%)	NPV (%)
$\Delta$ H69/V70	61.1 (5010)	99.9	75.4
N501Y	52.3 (5846)	100.0	99.9
E484K	0.6 (60)	97.7	100.0
L452R	35.9 (3441)	99.8	99.9

324 Mutation prevalence estimates were calculated based on consensus sequences from 9572 positive samples (as  
325 determined by E-Sarbeco PCR) obtained from this period.

326  
327  
328  
329  
330  
331  
332

In summary, we developed a RT-qPCR system for large-scale screening of four key mutations in parallel that is highly specific and sensitive, validated by a comparison of the qPCR and WGS data from 9572 samples that were tested in parallel.

## DISCUSSION

333 RT-qPCRs platforms for small and large-scale screening can support the detection of  
334 mutations of concern present in SARS-CoV-2 variants. This is of special interest for  
335 countries lacking an infrastructure for large-scale WGS sequencing, the golden  
336 standard for SARS-CoV-2 variant surveillance. Here, a detection system is needed  
337 that is fast, robust and flexible and, which enables the detection of known diagnostic  
338 mutations almost in real-time after sample collection, as we showed in this study.  
339 Here, we describe validated and advanced RT-qPCR platforms for small and large-  
340 scale screening that can simultaneously detect mutations of concern within the *S* of  
341 SARS-CoV-2, with a fast turnaround time for large-scale screening of 12-24h to  
342 report to the public health system. In comparison to commercially available systems  
343 to detect mutations of concern, the RT-qPCR platforms can be established fast and  
344 new mutations can be implemented; an important advantage to follow the course of a  
345 pandemic. It is a transparent system, where troubleshooting is possible without  
346 depending on the knowledge from a company and it can be adjusted to the existing  
347 infrastructure of the laboratory for large-scale screening and data evaluation.  
348 Moreover, the RT-qPCR platforms are at low cost of about 10 DKK (2 USD) per  
349 reaction, and can therefore be establish in countries without the resources for WGS in  
350 large-scale  
351 RT-qPCR is a fast, standard method for SARS-CoV-2 detection and has been  
352 established at the start of the pandemic in January 2020<sup>29</sup>. The standardised protocol  
353 for SARS-CoV-2 RT-qPCRs makes it easy to implement into diagnostic laboratories  
354 worldwide, where the equipment needed is commonly present. This could be of  
355 advantage compared to new methods such as RT-LAMP or CRISPR, which have  
356 been described for SARS-CoV-2 detection, delivering faster test results and can be  
357 applied without extensive laboratory equipment as RT-qPCRs<sup>33-35</sup>.  
358 Currently there are only limited studies on RT-LAMP for commercial point of care<sup>3</sup>.  
359 Moreover, CRISPR is still in its infancy<sup>36</sup> and has been shown to be less sensitive  
360 compared to RT-qPCR<sup>3</sup>. As most diagnostic facilities worldwide do not possess  
361 access and knowledge to establish these technologies, opposing to RT-qPCR that is a  
362 universal standard method, RT-qPCRs are still the method of choice for most  
363 diagnostic laboratories. Based on recent advances in modifications of conjugated-  
364 probes, RT-qPCRs can be designed to detect mutations within the SARS-CoV-2  
365 genome consisting out of a single nucleotide polymorphism (SNP).  
366 For small-scale screening the multiplexed RT-qPCR was developed using a Luna  
367 Probe One-Step RT-qPCR Mix, which offers the possibility to increase the input  
368 template concentration, for amplification targets with a low RNA concentration, as it  
369 is four times more concentrated. However, this was not an advantage when  
370 establishing the multiplexed RT-qPCRs **v.1** and **v.2**, as SARS-CoV-2 RNA  
371 concentrations vary among patient samples and can be too high from start leading to  
372 artificial signals. In contrast, adjusting the primer and probe concentrations for each  
373 mutation resulted in a highly specific and sensitive detection of the corresponding  
374 mutation present in the different SARS-CoV-2 variants (**Fig. 3J-O, Suppl. Tab. 4**).  
375 Moreover, by reducing the number of probes in the multiplexed RT-qPCR we could  
376 maintain a sensitive system for diagnostic use, by including one probes for each  
377 mutation. This was possible by designing and testing combinations of primer and  
378 MGB-, LNA- or BHQplus-conjugated probes that yield a specific signal for the  
379 mutation and WT sequences, respectively. The best performance for each  
380 primer/probe pairs is empirical and should be tested for all possible probe  
381 modifications (LNA, MGB and BHQplus), as the result is dependent on the  
382 nucleotide sequence of the mutation or WT sequence. So far, only mutations of



383 concern within the *S* were included into the multiplexed RT-qPCR platform for small-  
384 scale screening but running the  $\Delta$ H69/70 RT-qPCR as multiplexed PCR together with  
385 the clinical E-sarbeco RT-qPCR did not reduce the sensitivity of the PCR (**Fig. 2E**).  
386 As up to five targets can be included into the multiplex RT-qPCR using the Luna  
387 Probe One-Step RT-qPCR Mix, additional targets located in other loci of the SARS-  
388 CoV2 genome than *S* could be included. We did not test the maximum number of  
389 targets that could be included into RT-qPCR platform, as this was out of the scope of  
390 this study, but this could be of interest for future studies.

391 Large-scale RT-qPCR screening of mutations present in VOCs required that a number  
392 of technical and analytical considerations can be fulfilled: 1) the RT-qPCR must be  
393 highly specific and sensitive to minimise or avoid false positives, 2) it should be of  
394 sufficient robustness to allow for massive scalability required in a pandemic, 3) it  
395 must not interfere with the diagnostic PCR to detect SARS-CoV-2 to reduce the risk  
396 of potential PCR contamination 4) it requires liquid handlers in order to be viable  
397 from a practicable standpoint and 5) an advanced, automated evaluation system is  
398 needed to detect the erroneous results. Here we describe a large-scale RT-qPCR  
399 platform that meets the technical and analytical considerations outlined above. The  
400 current design is based on sample preparation in a 96-well format and subsequent RT-  
401 qPCR in 384-format. This allows each sample to be analysed by four separate sets of  
402 primers and probes, which enables the analysis of four mutations for up to 92 samples  
403 and four controls (one negative and three positive) in parallel in a single run. The  
404 system is flexible as the combination of target mutations can be adjusted over time in  
405 accordance with current needs. The handling of data calls for automated data  
406 processing and variant calling which is due the large amount of data in each run and  
407 the complex calling algorithms. Inconclusive results can pose a challenge with regards  
408 to variant calling. When one or more of the mutations are inconclusive, it is not  
409 always possible to make an unequivocal variant call. In our set-up we have opted to  
410 report the detected mutations. In these cases, prominent mutations with putative  
411 biological functions in various VOCs were reported, rather than variants of concern  
412 and interest.

413 From the large scale-screen it was determined that the RT-qPCR platform described  
414 in this study is generally of very high specificity and sensitivity and performs well in  
415 terms of its PPV and NPV, indicating its utility in such large-scale diagnostic screens.  
416 The period for the large-scale screening and validation was specifically chosen to  
417 interrogate the robustness of this system in a pandemic transition period with ongoing  
418 lineage replacement; such a period involves the waning of certain variants such as the  
419 Alpha (B.1.1.7) and its signature mutations  $\Delta$ H69/V70 and N501Y, along with the  
420 rise of a different variant like Delta (B.1.617.2) with a different signature mutation  
421 (L452R). In order to have diagnostic value, surveillance mechanisms which track  
422 these exclusive signatures, and which do not yield full genomes, must have adequate  
423 sensitivity and specificity to be able to adequately distinguish between such signature  
424 mutations (this is also aided by the E-Sarbeco PCR result, being the primary  
425 diagnostic method used to determine a SARS-CoV-2 infection). In that respect, the  
426 sensitivity and specificity of this system is excellent, only falling short in sensitivity in  
427 one assay ( $\Delta$ H69/V70) due to distinct technical issues, all of which revolve around the  
428 WGS reference standard and not the RT-qPCR itself. Firstly, the challenge of read  
429 alignment around genome deletions leads to ambiguous base-calls around these  
430 regions. Secondly, in large scale amplicon-based genomic surveillance, dropouts are  
431 not a rare occurrence, and a certain degree of N-counts is therefore considered  
432 permissible (typically less than 5-10 % of the consensus genome). Tracts of Ns

433 around this region were observed around the deletion and this was largely responsible  
434 for the challenges of identifying a deletion from WGS consensus genomes. However,  
435 this was not the case for single SNPs leading to non-synonymous substitutions as seen  
436 with N501Y, E484K and L452R. Interesting insights into the specificity and the  
437 sensitivity of the RT-qPCR system were also observed in the results around the  
438 L452R mutation, given that position L452 in the spike protein exhibited more than a  
439 single amino acid change during the pandemic and indeed the timeframe of the large-  
440 scale screening performed. The validation showed that all samples with L452Q in the  
441 spike protein recorded a positive result from the RT-qPCR whereas L452M  
442 exclusively recorded negative RT-qPCR results. Given that the codon observed from  
443 WGS encoding for Q was *cag* and the corresponding codon encoding for L at the  
444 same position was *cgg*, this could be considered unsurprising, also given that Q452  
445 was not an anticipated mutation and therefore was not considered in the design of the  
446 probes. Given that the codon *atg*, which is more distant from *cgg* and which encodes  
447 for M at this position, was not detected by the L452R-specific probe, this alludes to  
448 the specificity and sensitivity of the RT-qPCR probe at position 452.

449  
450 One of the major arms of pandemic control seen in this pandemic revolves around the  
451 screening and isolation of SARS-CoV-2 infected individuals in order to limit  
452 community spread of infections. The screening and isolation of individuals is  
453 therefore time sensitive and requires a rapid turnaround, especially where the control  
454 of variants or mutations of concern are a priority. While WGS of positive samples  
455 affords the accurate identification of these variants or mutations in order to enable  
456 their tracking and therefore control, this entails a longer turnaround time and greater  
457 cost in terms of reagents, equipment and expertise. The use of RT-qPCR systems such  
458 as the one described in this study allows for rapid identification of mutations of  
459 concern, which in turn enables near-real-time tracking of these and correspondingly,  
460 rapid decision-making around testing, contact tracing and isolation. This enabled the  
461 rapid reaction of the public health system in Denmark to the detection of VOCs, with  
462 the added benefit of gaining time to implement its vaccination schedule; being in line  
463 with modelling showing that minimising testing delay, had the largest impact on  
464 reducing onward transmissions<sup>37</sup>. The flexibility of this system also allows for  
465 multiplexing to detect multiple mutations and the incorporation of new primers and  
466 probes in response to the dynamics of the SARS-CoV-2 pandemic. In addition, the  
467 specificity and sensitivity of this system show that it is robust and therefore suited to  
468 diagnostic requirements in a pandemic. Taken together, these characteristics make this  
469 RT-qPCR system an ideal candidate for laboratories looking to detect mutations of  
470 concern in the SARS-CoV-2 pandemic. The current shift in our consideration of the  
471 pandemic (towards endemicity) suggests that such monitoring and screening might  
472 have to last a considerably longer time, making this system extremely viable in the  
473 long-term, and indeed in future outbreaks and pandemics.

474

475

476

477

478

479

480 **Material and Methods**

481

482 **Ethics**

483 Exemption for review by the ethical committee system and informed consent was  
484 given by the Committee on Biomedical Research Ethics - Capital region in  
485 accordance with Danish law on assay development projects.

486

487 **Virus isolation**

488 SARS-CoV-2 viral isolates representative of VOC (Delta variant B.1.617.2, Alpha  
489 variant B.1.1.7 and Beta variant B.1.351) were isolated from PCR-positive throat  
490 swabs collected in phosphate buffered saline (PBS) from community testing facilities  
491 (Test Center Denmark) and BioBank Denmark, which form part of the Danish  
492 national surveillance program<sup>4</sup>. The primary isolation was performed in 24-well  
493 culture plates with  $5 \times 10^4$  Vero E6 cells/well seeded the day before. Cells were washed  
494 once with PBS, and 150-250  $\mu$ L of swab material and 150-250  $\mu$ L infection media  
495 [Dulbecco's Modified Eagle Medium (DMEM) with 1% Penicillin/Streptomycin]  
496 were added to each well. After 1h incubation at 37°C/5% CO<sub>2</sub>, 1 mL/well of  
497 propagation media [DMEM with 1% Penicillin/Streptomycin, 5% foetal calf serum]  
498 was added, and the cultures were further incubated until cytopathic effect (CPE) was  
499 observed. Isolations performed later during the pandemic used additional 1.5  $\mu$ g/mL  
500 Amphotericin B in the propagation media. All cell culture reagents were obtained  
501 from Gibco, ThermoFisher Scientific, Waltham, MA, USA. Upon CPE, supernatants  
502 were aliquoted and frozen at -80°C. Subsequent passages to expand virus stocks were  
503 performed in 75 cm<sup>2</sup> flasks seeded with  $1.5 \times 10^6$  Vero E6 the day before. 25  $\mu$ L of  
504 primary isolate supernatant was used as inoculum in the presence of 2 mL infection  
505 media. After 1h at 37°C/5% CO<sub>2</sub> incubation, flasks were supplemented with 10 mL of  
506 propagation media (without Amphotericin) and incubated until CPE was obtained.  
507 Supernatants were then clarified by centrifugation for 5 min at 300 x g and stored as  
508 single use aliquots at -80°C.

509

510 **RT-qPCR validation standards and patient samples**

511 For determining specificity and sensitivity of the SARS-CoV-2 Variant PCR assays,  
512 the following materials were used:

513 Diagnostic samples positive for the common respiratory pathogens Human  
514 Coronavirus 229E, HKU1, NL63 and OC43, Adenovirus and Rhinovirus, was  
515 obtained as extracted nucleic acids from the human diagnostic Virus PCR laboratory  
516 at Statens Serum Institute, Denmark, and were all previously confirmed by PCR to be  
517 positive at high concentration (Ct <<30) for respective pathogens.

518 Extracted Influenza virus RNA from viruses cultured in Madin Darby Canine Kidney  
519 (MDCK) cells (A/Christchurch/16/2010(H1N1), pdm09-like virus,  
520 B/Phuket/3073/2013-like virus, B/Brisbane/60/2008-like virus, were all previously  
521 confirmed by PCR to be positive at high concentration (Ct <<30) for respective  
522 pathogens. The influenza reference viruses was provided by the WHO Collaborating  
523 Centre for Reference and Research on Influenza, The Francis Crick Institute,  
524 London, United Kingdom. Positive RNA controls for SARS-CoV-2 variants were  
525 obtained from extracted virus cultures and were diluted in DNase/RNase free water to  
526 generate CT values between 25-30 in the subsequent RT-qPCR.

527 TWIST Synthetic SARS-CoV-2 RNA controls (MT007544.1/Australia/VIC01/2020),  
528 (MT103907 England/205041766/2020), (MT104043 South African/KRISP-EC-  
529 K005299/2020) and (MT104044 Japan (IC-0564/2021) were bought from TWIST

530 bioscience and used as PCR standards WT, Alpha (B.1.17), Beta (B.1.351), Gamma  
531 (P.1), respectively.  
532 Selected SARS-CoV-2 VOC positive patient samples were obtained from the Danish  
533 National Biobank.

534

### 535 **Positive and Negative controls for the large-scale RT-qPCR platform**

536 Positive and negative controls for the large-scale platform were run in parallel with  
537 selected patient samples throughout extraction and RT-qPCR. DPBS 1x pH 7.2  
538 (Gibco) was used as negative control. Heat inactivated (56 °C for 45 min.) virus  
539 cultures, were used as positive control. Three Danish virus isolates were used to cover  
540 the four key mutations present in the Delta variant B.1.617.2 , Alpha variant B.1.1.7  
541 and Beta variant B.1.351 (SSI-H18).

542

### 543 **Nucleic acid extraction**

544 For small scale SARS-CoV-2 patient sample screening, total nucleic acid was  
545 extracted using a MagNApure96 extraction robot (Roche) with the MagNA Pure 96  
546 DNA and Viral NA Small Volume kit and the Viral NA Plasma SV protocol (200 µL  
547 input and 100 µL elution volume).

548 For positive controls, 120 µL of supernatant from SARS-CoV-2 infected cells were  
549 mixed with 120 µL of MagNA Pure lysis buffer (Roche) and extracted as small-scale  
550 SARS-CoV-2 patient samples. Positive control RNA was stored at -80°C until use.  
551 For large-scale SARS-CoV-2 patient sample screening, RNA was extracted using a  
552 Beckman Coulter Biomek i7 robot using the Beckman Coulter RNAdvance Whole  
553 blood kit (200 µL input and 50 µL elution volume).

554

### 555 **Primer and probe design**

556 SARS-CoV-2 variant sequences were retrieved from positive samples identified  
557 through the national surveillance program in Denmark. Sequences were aligned and  
558 primer and probes were designed using Geneious Prime 2021.0.  
559 Two probes were designed for each key mutation: one detecting the wildtype (WT)  
560 nucleotide sequence, and one detecting the mutation. The probe design was refined to  
561 detect the key mutations (L452R, E484K, N501Y, Δ69/V70 deletion) with only one  
562 probe in the multiplex RT-qPCRs. To ensure stable allelic discrimination analysis,  
563 probes detecting the mutations with only one nucleotide exchange were either MGB,  
564 LNA or BHQplus modified, which increases the melting temperature (T<sub>m</sub>). The  
565 calculation of MGB probe T<sub>m</sub> was adapted from<sup>38</sup>.

566

567 The primers and probes listed in Tab. 2 were synthesized by Biosearch Technologies,  
568 Denmark, except for the MGB-probes that were synthesized by Eurogentec, Belgium,  
569 and the Zen-probe, that was synthesized by Integrated DNA Technologies, Belgium.  
570 All oligos were HPLC-purified.

571

572

**Tab.2: Primer and probe sequences.**

Target	Primer/Probe name	T <sub>m</sub>	Primer/Probe sequence 5' – 3'	Volume (µL) <sup>(2)</sup>	Mix ID
<b>SARS-CoV-2 primary diagnostic assay:</b>					
E-gene	E_Sarbeco <sup>31</sup> _F	58.8	ACAGGTACGTTAATAGTTAATAGCGT	0.1	
	E_Sarbeco_R	61.0	ATATTGCAGCAGTACGCACACA	0.1	
	E_Sarbeco_P1	66.3	FAM-ACACTAGCCATCCTTACTGCGCTTCG-BHQ1	0.05	
<b>Key mutations primer and probes used in large scale testing:</b>					

<b>(Key mutations primers and probes used in small scale testing, see Mix ID)</b>					
ΔH69/V70	SARS-CoV-2 ΔH69/V70 F	58.5	ACATTCAACTCAGGACTTGTCT	0.1	1, 2, 5
	SARS-CoV-2 ΔH69/V70 R	58.0	TCATTAAATGGTAGGACAGGGTT	0.1	1, 2, 5
	SARS-CoV-2 ΔH69/V70 P <sup>(1)</sup>	61.2	HEX-TTCCATGCTATCTCTGGGACCA-BHQ2	0.05	1, 2, 5
N501Y	SARS-CoV-2 N501Y F	57.7	TGTTACTTTCCTTTACAATCATATGGT	0.1	1, 2, 5, 6
	SARS-CoV-2 N501Y R	58.9	TGCTGGTGCATGTAGAAGTTCA	0.1	1, 2, 5, 6
	SARS-CoV-2 501Y_mutant MGB P	64.8	FAM-CCCACTTATGGTGTGGT-MGB	0.05	2, 5, 6
	SARS-CoV-2 N501 WT MGB P	64.8	Cy5-CCCACTAATGGTGTGGT-MGB	0.05	2
E484K	SARS-CoV-2_E484K F	58.5	AGGAAGTCTAATCTCAAACCTTTTGA	0.1	3, 5, 6
	SARS-CoV-2_E484K R	60.2	GTCCACAAACAGTTGCTGGTG	0.1	3, 5, 6
	SARS-CoV-2_484K_mutant MGB FAM P	64.6	FAM-TGGTGTAAAGGTTTTAAT-MGB	0.05	3
	SARS-CoV-2_E484K_WT MGB P	63.5	Texas Red-TGGTGTGAAGGTTTTAA-MGB	0.05	3
L452R	SARS-CoV-2_L452R F	60.5	CAGGCTGCGTTATAGCTTGA	0.1	4, 6
	SARS-CoV-2_L452R R	57.1	CCGGCCTGATAGATTTCAGT	0.1	4, 6
	SARS-CoV-2_452R_mutant BHQ+ P	58.2	HEX-TATAATTACCGGTATAGATTGTT-BHQ1	0.05	4, 6
	SARS-CoV-2_L452_WT BHQ+ P	58.0	Cal Fluor Red 610-TATAATTACCTGTATAGATTGTTA-BHQ2	0.05	4
<b>Key mutation probes used in first version of N501Y assay, used in large scale testing:</b>					
N501Y	SARS-CoV-2 501Y_mutant LNA P	63.2	FAM -CCCAC+T+T+ATGG+TGTTGGT-BHQ1	0.05	1
	SARS-CoV2 N501 WT LNA P	62.6	Quasar 670-CCCAC+T+A+ATGG+TGTTGGT-BHQ2	0.05	1
<b>Key mutation probes used exclusively in multiplex RT-qPCR in small scale testing:</b>					
ΔH69/V70	SARS-CoV-2 ΔH69/V70 Zen P	61.2	HEX-TTCCATGCT/ZEN/ATCTCTGGGACCA-IABkFQ	0.05	5
E484K	SARS-CoV-2_484K_mutant MGB Cy5 P	64.6	Cy5-TGGTGTAAAGGTTTTAAT-MGB	0.15	5, 6

573

574

575 **LNA = Locked Nucleic Acid, a “+” before a nucleotide indicates position of LNA modified base,**  
576 **MGB = Minor Groove Binder, BHQ+ = BHQplus modified probe. Mastermix ID indicates which**  
577 **primer and probes were used in the same mastermix. SNP mutations are marked in bold.**

577

578

(1) While it is more common to use a BHQ1 quencher together with HEX, this system works well with a BHQ2 quencher.

579

(2) Volumes of oligos added to mastermix are valid for both 96 and 384-well formats.

580

581

### Mastermix set-up

582

The primers and probes were combined in different master-mixes.

583

In master-mix 1-4 (large-scale screening): the mutations were detected using both the mutant probe and the wildtype probe for allelic discrimination analysis.

584

585

In master-mix 5 and 6 (small-scale screening), only probes targeting the mutations were used, and therefore no allelic discrimination analysis was needed.

586

587

588

### 96-well format PCR conditions used in development phase and small-scale testing

589

All PCR assays were developed on a Bio-Rad CFX 96 PCR real-time PCR system.

590

**Master-mix 1 - 4** contained 12.5 μL Luna<sup>®</sup> Universal Probe One-step RT-qPCR Kit

591

reaction buffer (NEB), 1.25 μL Luna<sup>®</sup> WarmStart RT Enzyme mix, primers and

592

probes (100 μM, volumes in table 1), DNase/RNase free water and 5 μL template to

593 a total volume of 25  $\mu$ L. Cycling conditions: Reverse transcription at 55  $^{\circ}$ C for 10  
594 min., initial denaturation at 95  $^{\circ}$ C for 3 min., followed by 45 cycles of denaturation  
595 and annealing/extension at 95  $^{\circ}$ C for 15 sec. and 58  $^{\circ}$ C at 30 sec. respectively.  
596 **Master-mix 5 - 6** contained 5  $\mu$ L Luna Probe One-Step RT-qPCR 4X Mix with UDG  
597 (New England Biolabs Inc (NEB)), primers and probes (100  $\mu$ M, volumes in Tab. 1),  
598 DNase/RNase free water and 5 $\mu$ L template to a total volume of 25  $\mu$ L. Cycling  
599 conditions: Initial step at 25 $^{\circ}$ C for 30 sec, reverse transcription at 55  $^{\circ}$ C for 10 min.,  
600 initial denaturation at 95  $^{\circ}$ C for 1 min., followed by 45 cycles of denaturation and  
601 annealing/extension at 95 $^{\circ}$ C for 10 sec and 58 $^{\circ}$ C at 60 sec respectively.

602

#### 603 Data analysis for the multiplexed RT-qPCRs used in small-scale testing

604 The multiplexed RT-qPCRs contain probes only targeting the mutations,  $\Delta$ H69/V70,  
605 501Y, 484K for **master-mix 5**, and 501Y, 484K, 452R for **master-mix 6**. Cut-off  
606 values were used in the multiplexed RT-qPCRs to secure the detection of only the  
607 mutation and not the WT sequence as there was no WT probe in the mix. A sample  
608 was considered positive with these criteria: Ct <38 and RFU (Relative Fluorescence  
609 Units) > 500 at Ct = 45.

610

#### 611 384-well format PCR conditions for large-scale testing

612 In large scale testing, the assays run on a Bio-Rad CFX 384 PCR real-time PCR  
613 system. The master-mix contained 7.5  $\mu$ L Luna<sup>®</sup> Universal Probe One-step RT-qPCR  
614 Kit reaction buffer (New England Biolabs Inc), 0.75  $\mu$ L Luna<sup>®</sup> WarmStart RT  
615 Enzyme mix, primers and probes (100  $\mu$ M, volumes in table 1), DNase/RNase free  
616 water and 5 $\mu$ L template to a total volume of 15  $\mu$ L. Cycling conditions were the same  
617 as for the 96-well format. Each patient sample was analysed in four PCR wells, in  
618 four parallel reactions, using master-mix 1 or 2 for detecting  $\Delta$ H69/V70 and N501Y,  
619 master-mix 3 for detecting E484K, master-mix 4 for detecting L452R and in the final  
620 well the E-Sarbeco assay was used for detection of SARS-CoV-2 wildtype (E-gene).  
621 The 4 master-mixes were placed in a quadratic pattern, thus allowing easy transfer  
622 from a 96-well plate to a 384-well plate (e.g. A1 in a template plate was pipetted to  
623 A1, B1, A2 and B2 of the master mix plate). Master-mix 5 and 6 were not tested in  
624 the 384-well format.

625

#### 626 Data analysis using allelic discrimination analysis in large-scale testing

627 PCR curves were evaluated in the Bio-RAD CFX software and Ct values and end  
628 RFU were exported in csv files. The files were imported into the laboratory database  
629 where all data analysis was performed. For the  $\Delta$ H69/V70 deletion, detection was  
630 based on Ct values (deletion detected is Ct = 12-38). For the the mutations N501Y,  
631 E484K and L452R, detection was based on allelic discrimination where the end RFU  
632 values were utilized to determine the presence of a mutation (see Suppl. Tab. 1). A  
633 sample was considered positive with these criteria: Ct <38 and RFU > 200 at Ct = 45.  
634 The RFU cut-off value was used in the 384-well PCR-format as a quality control step,  
635 in case one of the probes in the allelic discrimination pair failed.

636

#### 637 Whole genome sequencing

638 Whole genome sequences were generated by The Danish COVID-19 Genome  
639 Consortium (DCGC) from PCR-positive samples collected between 6<sup>th</sup> June and 11<sup>th</sup>  
640 July 2021. Samples were selected using Ct cut off values between 30 – 38<sup>30</sup>. The bulk  
641 of the samples were sequenced using the ARTIC Network tiled PCR scheme V3 via  
642 the COVIDseq Assay [Illumina], Artic Network nCoV-2019 sequencing protocol v2

643 ([dx.doi.org/10.17504/protocols.io.bdp7i5rn](https://doi.org/10.17504/protocols.io.bdp7i5rn) [Oxford Nanopore], or a custom DCGC  
644 protocol ([dx.doi.org/10.17504/protocols.io.bfc3jiyn](https://doi.org/10.17504/protocols.io.bfc3jiyn))[Oxford Nanopore], adapted from  
645 the Artic Network protocol. Data pre-processing and consensus genome generation  
646 was performed using Illumina-specific ([github.com/connor-lab/ncov2019-artic-nf](https://github.com/connor-lab/ncov2019-artic-nf), v.  
647 1.3.0) or Oxford Nanopore-specific ([github.com/artic-network/fieldbioinformatics](https://github.com/artic-network/fieldbioinformatics), v.  
648 1.2.1) consensus pipelines. Consensus genome mutation calling with reference to  
649 Wuhan-Hu-1/2019 (Genbank Accession: MN908947) was performed with Nextclade  
650 CLI ([github.com/nextstrain/nextclade](https://github.com/nextstrain/nextclade), v. 1.2.0) and lineage designations were  
651 performed using pangolin ([github.com/cov-lineages/pangolin](https://github.com/cov-lineages/pangolin), v. 3.1.3) with the  
652 accompanying pangoLEARN model ([github.com/cov-lineages/pangoLEARN](https://github.com/cov-lineages/pangoLEARN), v.  
653 1.2.6).

654  
655

### 656 RT-qPCR Validation

657

658 Nucleotide sequences corresponding to the Sof consensus genomes derived from  
659 WGS were aligned using the MAFFT version 7.480 ([mafft.cbrc.jp](http://mafft.cbrc.jp)), utilizing the FFT-  
660 NS-2 algorithm with a maximum of 1000 iterations<sup>40,41</sup>. Alignments were viewed and  
661 processed in Jalview 2.11.1.4 ([jalview.org](http://jalview.org),<sup>42</sup>) and codons encoding key mutations  
662 were extracted, translated and compared to RT-qPCR results. From here, sensitivity,  
663 specificity, Positive Predictive Values (PPV) and Negative Predictive Values (NPV)  
664 were calculated for each set of primers and probes used in RT-qPCR assays. Positive  
665 and Negative Predictive Values were calculated according to the following formulas:  
666

$$667 \quad PPV = \frac{Sen * Prev}{(Sen * Prev) + (1 - Spec) * (1 - Prev)} \quad NPV = \frac{Spec * (1 - Prev)}{Spec * (1 - Prev) + (1 - Sen) * Prev}$$

668

669 where *Sen* = sensitivity, *Spec* = specificity and *Prev* = prevalence calculated from  
670 WGS consensus genomes. All analyses were performed in Rstudio version 1.4.1717  
671 using R version 4.1.1 and using the packages *tidyverse* (1.3.1), *seqinr* (4.2-8),  
672 *lubridate* (1.7.10), *ggplot2* (3.3.4), *cowplot* (1.1.1), *zoo* (1.8-9) and *ggpubr* (0.4.0).

673

### 674 DATA analysis

675

676 We used standard curves to determine the SARS-CoV-2 detection threshold for each  
677 assay and to calculate the viral load in each sample. We used the SARS-CoV-2  
678 variant specific TWIST control with a known concentration (copies/ $\mu$ l) and diluted  
679 1:10 in a seven-step dilution series. The median Ct-values and the interquartile ranges  
680 were calculated based on biological duplicates with technical duplicates. The  
681 threshold was based on the intercept of the linear regression line of the standard  
682 dilutions. Furthermore, the number of virus particles were estimated based on the  
683 logarithmic regression function of each assay's standard dilution series.

684

## 685 **Figure legends**

686

687 **Figure 1. Overview of the key mutations located in the spike glycoprotein during**  
688 **the pandemic and PCR strategies. (A)** The spike glycoprotein is located between  
689 the ORF1B and 2a within the SARS-CoV-2 genome. The  $\Delta$ H69/V70 (2 amino acid  
690 deletion) is located in the N-terminal domain (NTD) of the spike glycoprotein and the  
691 L452R, E484K and N501Y mutations are located in the receptor-binding domain

692 (RBD). Sets of four variant specific mutations present in VOC. The Beta (B.1.351)  
693 and the Gamma (P.1) have the same key mutations. The  $\gamma$  mutations are also present  
694 SARS-CoV2 variants that are not variants of concern, but the variants are included  
695 into this study for detecting the mutations in patient samples. **B)** Prevalence of spike  
696 mutations  $\Delta$ H69/V70, N501Y, E484K, L452R amongst SARS-CoV-2 consensus  
697 genomes in Denmark between 7<sup>th</sup> of June 2021 to the 11<sup>th</sup> of July 2021 **(C)** Variant  
698 composition (by Pangolin nomenclature) harbouring key spike mutations.

699 **Figure 2 Schematic overview about the PCR platforms and establishment of the**  
700 **H69/70 RT-qPCR.** **(A)** Multiplexed RT-qPCR v.1 targeting  $\Delta$ H69/70V, E484K- and  
701 N501Y mutation. The deletion and mutations are detected with one probe respectively  
702 and the E484K and N501Y mutations are detected by one primer pair resulting in a  
703 single amplification product for both mutations. **(B)** As proof of concept  $\Delta$ H69/70V  
704 was replaced by the L452R mutation of the delta variant (B.1.617.2) in the  
705 multiplexed RT-qPCR v.2. **(C)** A HEX-labelled probe detects the  $\Delta$ H69/70 and **(D)** a  
706 FAM-labelled probe the WT nucleotide sequence. **(E)** Dilution row of the TWIST  
707 control (WT SARS-CoV-2) to detect the limit of detection **(F)** Detection of the  
708  $\Delta$ H69/V70 (red bars) or WT sequence (blue bars) in positive SARS-CoV-2 patient  
709 samples. The positive control (patient sample with the  $\Delta$ H69/V70) is displayed as  
710 green bar and the negative control as grey bar. **(G)** Prevalence of top ten SARS-CoV-  
711 2 variants in Denmark (based on pangolin lineage assignments using WGS-derived  
712 consensus genomes) from 12<sup>th</sup> Jan 2021 to 8<sup>th</sup> Mar 2021. **(I)** Large scale screening of  
713 positive SARS-CoV-2 patient samples in the  $\Delta$ H69/70 RT-qPCR in the period from  
714 12<sup>th</sup> of Jan to the 8<sup>th</sup> of March 2021 **(H)** Frequency of  $\Delta$ H69/70V and N501Y  
715 mutations in Denmark from 12<sup>th</sup> Jan to 8<sup>th</sup> Mar 2021, as determined from WGS  
716 consensus genomes obtained in this period. Mutations are relative to Wuhan-Hu-  
717 1/2019 (Genbank Accession: MN908947). Arrow bars in **E** and **F** indicate SEM for  
718 two technical replicates.

719 **Figure 3 Primer and probes performance for the L452R, E484K and N501Y**  
720 **mutations and screening of patient samples positive for SARS-CoV-2 with**  
721 **different mutations of concern present in the multiplexed RT-qPCRs v.1 and v.2**  
722 **A-B)** BHQplus-conjugated probes detecting the L452 WT SARS-CoV-2 nucleotide  
723 sequence the 452R mutation. **C)** Dilution row of a patient sample with known whole  
724 genome sequence information for the delta variant (B.1.617.2) tested in parallel in the  
725 L452R- and E-sarbeco RT-qPCR. **D)** MGB-conjugated probes detecting the E484  
726 WT SARS-CoV-2 nucleotide sequence and the 484K mutation. **F)** Dilution row of the  
727 TWIST control (Gamma P.1) included into the E484K RT-qPCR. **G)** MGB-  
728 conjugated probe detecting the N501 WT SARS-CoV-2 nucleotide sequence and the  
729 Y501 mutation. **I)** Dilution row of the TWIST control (Alpha B.1.1.7) included into  
730 the N501Y RT-qPCR. **J-L)** Detection of three key mutations  $\Delta$ H69/V70, E484K and  
731 N501Y in patient samples with known whole genome sequence information identified  
732 as Alpha (B.1.1.7), Beta (B.1.351) and P.2 variants by the multiplexed RT-qPCR **v.1.**  
733 **M-O)** Detection of three key mutations L452R, E484K and N501Y in patient samples  
734 with known whole genome sequence information identified as Alpha (B.1.1.7), Beta  
735 (B.1.351) and Delta (B.1.617.2) variants by the multiplexed RT-qPCR **v.2.** Arrow  
736 bars in **C**, **F** and **I** indicate SEM for two technical replicates.



737 **Figure 4 Large scale screening of four key mutations.** A) Schematic overview of  
738 large-scale screening. B) Primer and probes included into the multiplexed and single  
739 PCR running in the 384-well plate format. C) RT-qPCR results from large-scale  
740 screening for each target mutation: E484K (upper left), L452R (upper right), N501Y  
741 (lower left),  $\Delta$ H69/70V (lower right) shown as positive (POS, green), negative (NEG,  
742 blue) or inconclusive (INK, grey).

743 **Figure 5 Validation of RT-qPCR results from large-scale screening.** Concordance  
744 between RT-qPCR results and WGS results represented as a graphical matrix with  
745 each cell represented as a circle showing the number of samples which correspond to  
746 a positive (POS, green) or negative (NEG, blue) RT-qPCR result (horizontal axis) and  
747 a given amino acid derived from WGS consensus genomes (vertical axis) for E484K  
748 (upper left panel), L452R (upper right panel), N501Y (lower left panel),  $\Delta$ H69/70V  
749 (lower right panel). Sensitivity and specificity for each RT-qPCR shown at bottom  
750 right of each panel.

751 **Supplementary Figure 1 Detection of the H69/70V deletion by RT-qPCR.** A-C)  
752 Detection of the  $\Delta$ H69/V70 in patient sample with known whole genome sequence  
753 information identified as Alpha (B.1.1.7), B.1.258 and B.1.298 variants (red bars).  
754 Positive control (green bar) of sample with known sequence information positive for  
755 the  $\Delta$ H69/70 and the negative control (grey bar). D) Prevalence of all SARS-CoV-2  
756 variants in Denmark (based on pangolin lineage assignments using WGS-derived  
757 consensus genomes) from 12<sup>th</sup> Jan 2021 to 8<sup>th</sup> Mar 2021. E) Dilution of the TWIST  
758 control (WT SARS-CoV-2) and detection of the H69/V70 WT sequence by the  
759 H69/V70 RT-qPCR or the multiplexed H68/V70\_E-sarbeco RT-qPCR. Arrow bars in  
760 E indicate SEM for two technical replicates.

761 **Supplementary Figure 2 LNA-modified probes detecting the N501Y mutation.**  
762 A-B) LNA probes detecting the 501Y mutation and N501 WT sequence respectively.  
763 C) Allelic discrimination analysis to differentiate between the 510Y mutation and  
764 N501WT sequence. D) Multiplexed PCR to detect the  $\Delta$ H69/V70 mutation and the  
765 N501Y mutation.

## 766 **Acknowledgements**

767 We would like to extend our gratitude to Susanne Lopez Rasmussen and Halenur A.  
768 Bayhan for their assistance and technical support. We would like to acknowledge the  
769 originating laboratories and WHO Collaborating Centre for Reference and Research  
770 on Influenza, The Francis Crick Institute, London, United Kingdom for providing  
771 reference virus material.

772

## 773 **Author contributions**

774 Conceptualization: K.S., V.G., E.M., A.A.N., S.M., M.R., R.L., M.W.R., C.P., J.F.,  
775 A.S.C, C.N. and A.F. Methodology: K.S., V.G., E.M., S.H.N., C.P., M.G.P.J, L.N.  
776 and DCGC. Investigation/Analysis: K.S., V.G., S.M.K., M.R., J.F. and A.S.C  
777 Visualization and data curation: K.S, V.G, E.M., A.A.N. and J.F.  
778 Supervision: A.F., A.S.C and C.P. Writing original draft: K.S. V.G. and A.F. Writing  
779 reviewing/editing: K.S., V.G., E.M., S.H.N., M.J., A.S.F., L.N., A.A.N., S.M.K.,  
780 DCGC., S.M., M.R., R.L., M.W.R., C.P., J.F., A.S.C., C.N. and A.F. All authors  
781 critically revised the manuscript for important intellectual content and gave final  
782 approval for the submitted version.

783

784 **Conflict of interest**

785 The authors declare no competing interests

786

787 **REFERENCES**

788

- 789 1. Gravagnuolo, A. M. *et al.* High throughput diagnostics and dynamic risk  
790 assessment of SARS-CoV-2 variants of concern. (2021)  
791 doi:10.1016/j.ebiom.2021.103540.
- 792 2. SARS-CoV-2 variants of concern as of 16 September 2021.  
793 <https://www.ecdc.europa.eu/en/covid-19/variants-concern>.
- 794 3. Graham, M. *et al.* Use of emerging testing technologies and approaches for  
795 SARS-CoV-2: review of literature and global experience in an Australian  
796 context. *Pathology* **53**, 689 (2021).
- 797 4. Lyngse, F. P. *et al.* Association between SARS-CoV-2 Transmissibility, Viral  
798 Load, and Age in Households. *medRxiv* 2021.02.28.21252608 (2021)  
799 doi:10.1101/2021.02.28.21252608.
- 800 5. Campbell, F. *et al.* Increased transmissibility and global spread of SARS-CoV-  
801 2 variants of concern as at June 2021. *Eurosurveillance* **26**, 1–6 (2021).
- 802 6. A, S., J, M., B, T. & C, R. SARS-CoV-2 Delta VOC in Scotland:  
803 demographics, risk of hospital admission, and vaccine effectiveness. *Lancet*  
804 (*London, England*) **397**, 2461–2462 (2021).
- 805 7. Dejnirattisai, W. *et al.* Antibody evasion by the P.1 strain of SARS-CoV-2.  
806 *Cell* **184**, 2939-2954.e9 (2021).
- 807 8. Funk, T. *et al.* Characteristics of SARS-CoV-2 variants of concern B.1.1.7,  
808 B.1.351 or P.1: data from seven EU/EEA countries, weeks 38/2020 to 10/2021.  
809 *Eurosurveillance* **26**, 2100348 (2021).
- 810 9. SA, M. *et al.* Efficacy of the ChAdOx1 nCoV-19 Covid-19 Vaccine against the  
811 B.1.351 Variant. *N. Engl. J. Med.* **384**, 1885–1898 (2021).
- 812 10. Pearson, C. A. Estimates of severity and transmissibility of novel South Africa  
813 SARS-CoV-2 variant 501Y.V2. 1.
- 814 11. Cele, S. *et al.* Escape of SARS-CoV-2 501Y.V2 from neutralization by  
815 convalescent plasma. *Nat.* 2021 5937857 **593**, 142–146 (2021).
- 816 12. Faria, N. R. *et al.* Genomics and epidemiology of the P.1 SARS-CoV-2 lineage  
817 in Manaus, Brazil. *Science* (80-. ). **372**, 6544 (2021).
- 818 13. SARS-CoV-2 variants of concern and variants under investigation in England.
- 819 14. Stowe, J. *et al.* Effectiveness of COVID-19 vaccines against hospital admission  
820 with the Delta (B.1.617.2) variant.
- 821 15. Welcome - Knowledge Hub.  
822 [https://khub.net/welcome?p\\_p\\_state=normal&p\\_p\\_mode=view&saveLastPath=false&\\_com\\_liferay\\_login\\_web\\_portlet\\_LoginPortlet\\_mvcRenderCommandName=%2Flogin%2Flogin&p\\_p\\_id=com\\_liferay\\_login\\_web\\_portlet\\_LoginPortlet&p\\_p\\_lifecycle=0&\\_com\\_liferay\\_login\\_web\\_portlet\\_LoginPortlet\\_redirect=%2Fdocuments%2F135939561%2F430986542%2FEffectiveness%2Bof%2BCOVID-19%2Bvaccines%2Bagainst%2Bthe%2BB.1.617.2%2Bvariant.pdf%2F204c11a4-e02e-11f2-db19-b3664107ac42](https://khub.net/welcome?p_p_state=normal&p_p_mode=view&saveLastPath=false&_com_liferay_login_web_portlet_LoginPortlet_mvcRenderCommandName=%2Flogin%2Flogin&p_p_id=com_liferay_login_web_portlet_LoginPortlet&p_p_lifecycle=0&_com_liferay_login_web_portlet_LoginPortlet_redirect=%2Fdocuments%2F135939561%2F430986542%2FEffectiveness%2Bof%2BCOVID-19%2Bvaccines%2Bagainst%2Bthe%2BB.1.617.2%2Bvariant.pdf%2F204c11a4-e02e-11f2-db19-b3664107ac42)
- 830 16. Volz, E. *et al.* Transmission of SARS-CoV-2 Lineage B.1.1.7 in England:  
831 Insights from linking epidemiological and genetic data.

- 832 doi:10.1101/2020.12.30.20249034.
- 833 17. TN, S. *et al.* Deep Mutational Scanning of SARS-CoV-2 Receptor Binding  
834 Domain Reveals Constraints on Folding and ACE2 Binding. *Cell* **182**, 1295-  
835 1310.e20 (2020).
- 836 18. Zhou, R. *et al.* Viral dynamics in asymptomatic patients with COVID-19. *Int.*  
837 *J. Infect. Dis.* **96**, 288–290 (2020).
- 838 19. Y, W. *et al.* Escape from neutralizing antibodies by SARS-CoV-2 spike protein  
839 variants. *Elife* **9**, 1 (2020).
- 840 20. TN, S. *et al.* Prospective mapping of viral mutations that escape antibodies  
841 used to treat COVID-19. *Science* **371**, 850–854 (2021).
- 842 21. Harvey, W. T. *et al.* SARS-CoV-2 variants, spike mutations and immune  
843 escape. doi:10.1038/s41579-021-00573-0.
- 844 22. Liu, Z. *et al.* Identification of SARS-CoV-2 spike mutations that attenuate  
845 monoclonal and serum antibody neutralization. *Cell Host Microbe* **29**, 477-  
846 488.e4 (2021).
- 847 23. AJ, G. *et al.* Comprehensive mapping of mutations in the SARS-CoV-2  
848 receptor-binding domain that affect recognition by polyclonal human plasma  
849 antibodies. *Cell Host Microbe* **29**, 463-476.e6 (2021).
- 850 24. Boklund, A. *et al.* Monitoring of SARS-CoV-2 infection in mustelids. *EFSA J.*  
851 **19**, (2021).
- 852 25. Hammer, A. S. *et al.* SARS-CoV-2 transmission between mink (neovison  
853 vison) and Humans, Denmark. *Emerg. Infect. Dis.* **27**, 547–551 (2021).
- 854 26. Lassaunière, R. *et al.* In vitro Characterization of Fitness and Convalescent  
855 Antibody Neutralization of SARS-CoV-2 Cluster 5 Variant Emerging in Mink  
856 at Danish Farms. *Front. Microbiol.* **0**, 1679 (2021).
- 857 27. Özkan, E. *et al.* High-throughput Mutational Surveillance of the SARS-CoV-2  
858 Spike Gene. *medRxiv* 2021.07.22.21259587 (2021)  
859 doi:10.1101/2021.07.22.21259587.
- 860 28. Jørgensen, T. S. *et al.* A rapid, cost efficient and simple method to identify  
861 current SARS-CoV-2 variants of concern by Sanger sequencing part of the  
862 spike protein gene. *medRxiv* 2021.03.27.21252266 (2021)  
863 doi:10.1101/2021.03.27.21252266.
- 864 29. VM, C. *et al.* Detection of 2019 novel coronavirus (2019-nCoV) by real-time  
865 RT-PCR. *Euro Surveill.* **25**, (2020).
- 866 30. Michaelsen, T. Y. *et al.* Introduction and transmission of SARS-CoV-2 B.1.1.7  
867 in Denmark. *medRxiv* 2021.06.04.21258333 (2021)  
868 doi:10.1101/2021.06.04.21258333.
- 869 31. Li, B. *et al.* Viral infection and transmission in a large, well-traced outbreak  
870 caused by the SARS-CoV-2 Delta variant. *medRxiv* 2021.07.07.21260122  
871 (2021) doi:10.1101/2021.07.07.21260122.
- 872 32. Trevethan, R. Sensitivity, Specificity, and Predictive Values: Foundations,  
873 Pliabilities, and Pitfalls in Research and Practice. *Front. Public Heal.* **0**, 307  
874 (2017).
- 875 33. Huang, W. E. *et al.* RT-LAMP for rapid diagnosis of coronavirus SARS-CoV-  
876 2. *Microb. Biotechnol.* **13**, 950–961 (2020).
- 877 34. Lim, B. *et al.* Clinical validation of optimised RT-LAMP for the diagnosis of  
878 SARS-CoV-2 infection. *Sci. Reports* 2021 111 **11**, 1–11 (2021).
- 879 35. Broughton, J. P. *et al.* CRISPR–Cas12-based detection of SARS-CoV-2. *Nat.*  
880 *Biotechnol.* 2020 387 **38**, 870–874 (2020).
- 881 36. Mustafa, M. I. & Makhawi, A. M. Sherlock and detectr: CRISPR-cas systems

- 882 as potential rapid diagnostic tools for emerging infectious diseases. *J. Clin.*  
883 *Microbiol.* **59**, (2021).
- 884 37. Kretzschmar, M. E. *et al.* Impact of delays on effectiveness of contact tracing  
885 strategies for COVID-19: a modelling study. *Lancet. Public Heal.* **5**, e452  
886 (2020).
- 887 38. Afonina, I. *et al.* Efficient priming of PCR with short oligonucleotides  
888 conjugated to a minor groove binder. *Nucleic Acids Res.* **25**, 2657 (1997).
- 889 39. Tyson, J. R. *et al.* Improvements to the ARTIC multiplex PCR method for  
890 SARS-CoV-2 genome sequencing using nanopore. *bioRxiv* **3**, 1 (2020).
- 891 40. Katoh, K. & Standley, D. M. MAFFT Multiple Sequence Alignment Software  
892 Version 7: Improvements in Performance and Usability. *Mol. Biol. Evol.* **30**,  
893 772 (2013).
- 894 41. K, K., K, M., K, K. & T, M. MAFFT: a novel method for rapid multiple  
895 sequence alignment based on fast Fourier transform. *Nucleic Acids Res.* **30**,  
896 3059–3066 (2002).
- 897 42. Waterhouse, A. M., Procter, J. B., Martin, D. M. A., Clamp, M. & Barton, G. J.  
898 Jalview Version 2—a multiple sequence alignment editor and analysis  
899 workbench. *Bioinformatics* **25**, 1189–1191 (2009).
- 900  
901

# Figure 1

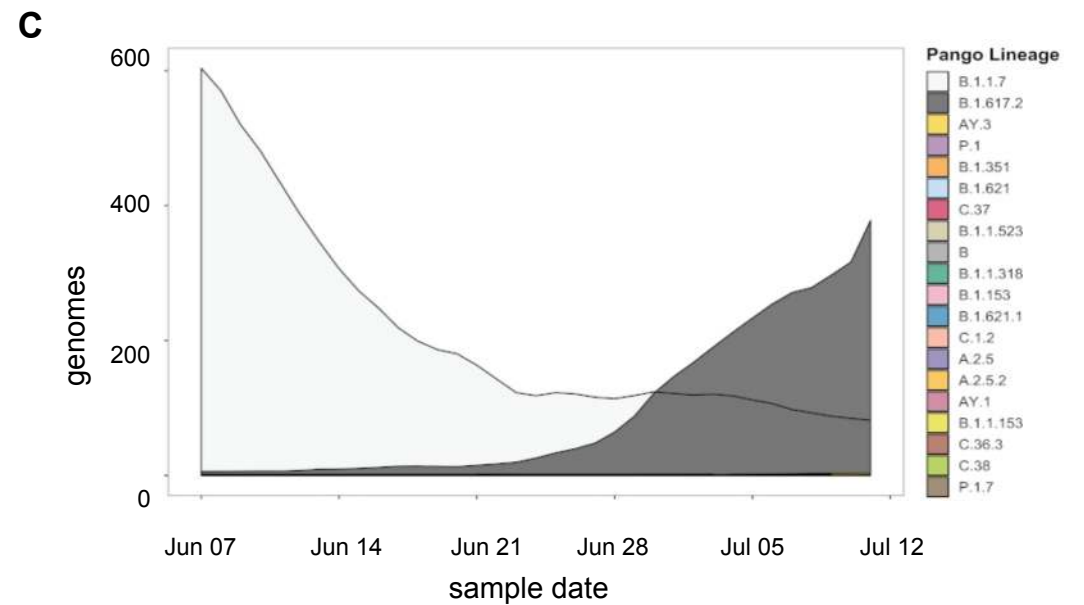
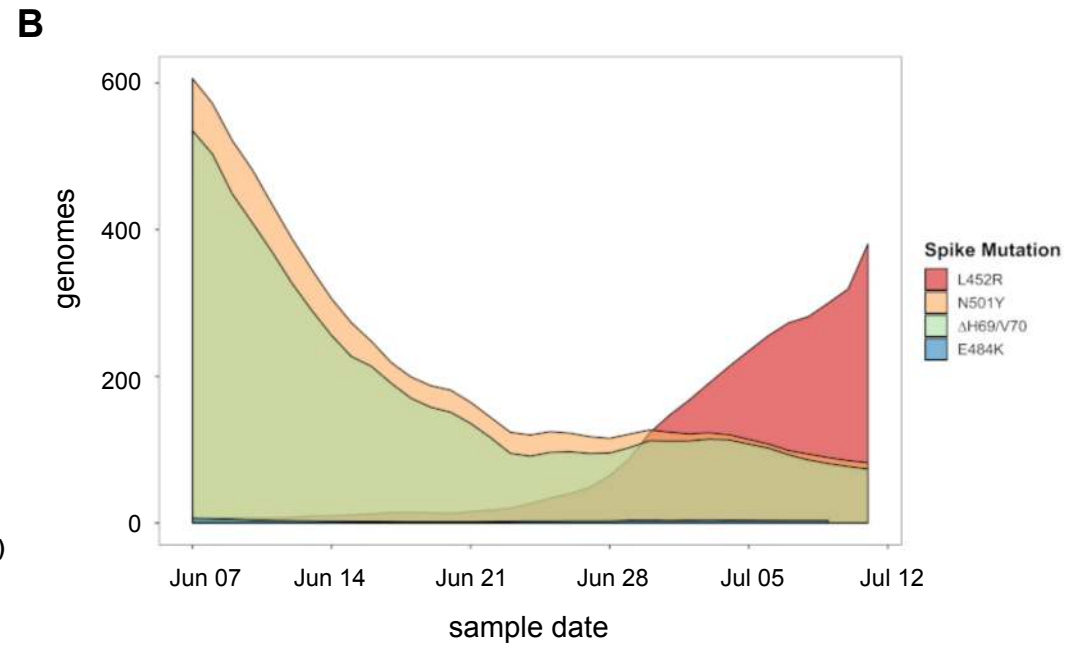
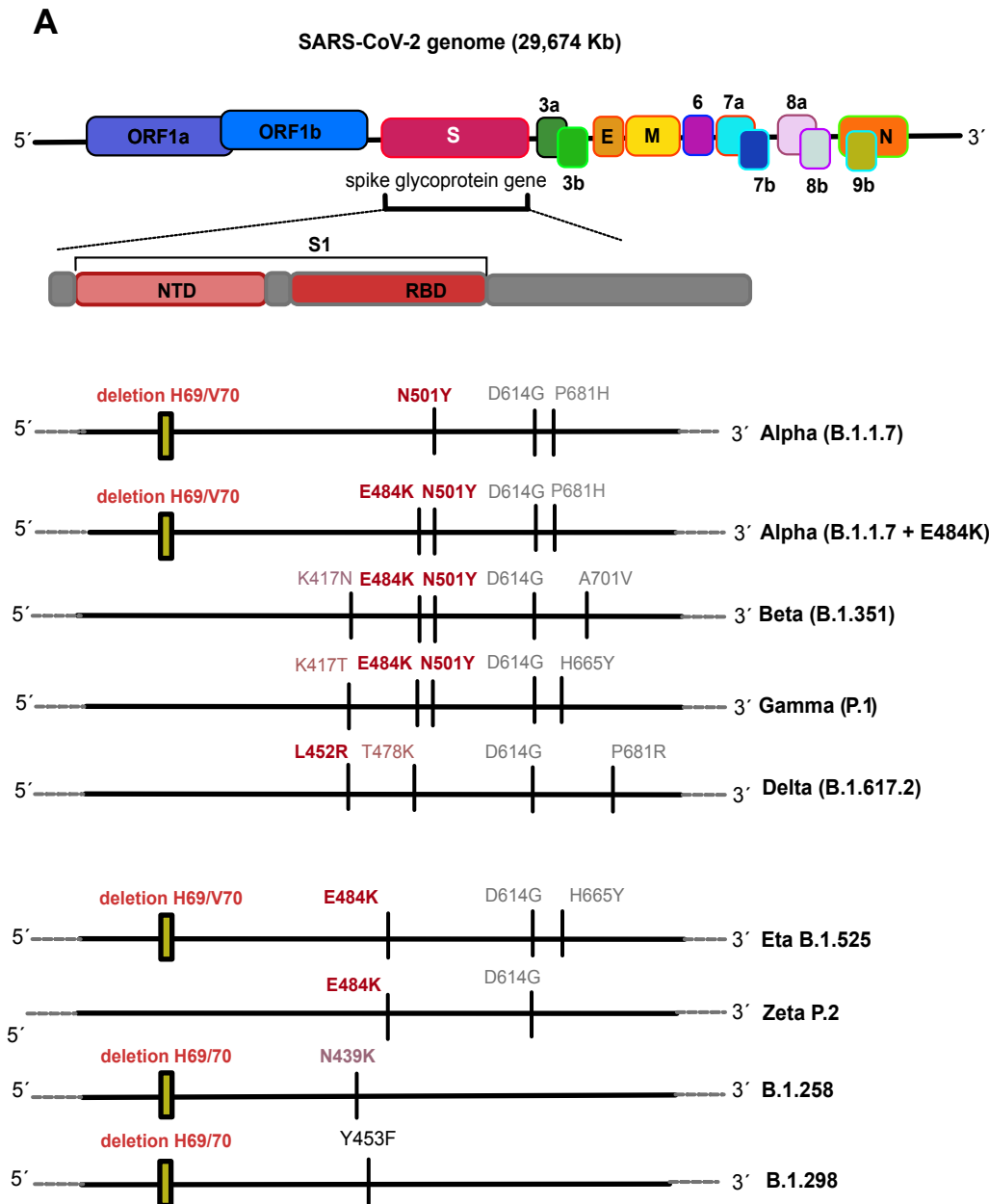


## Figure 2

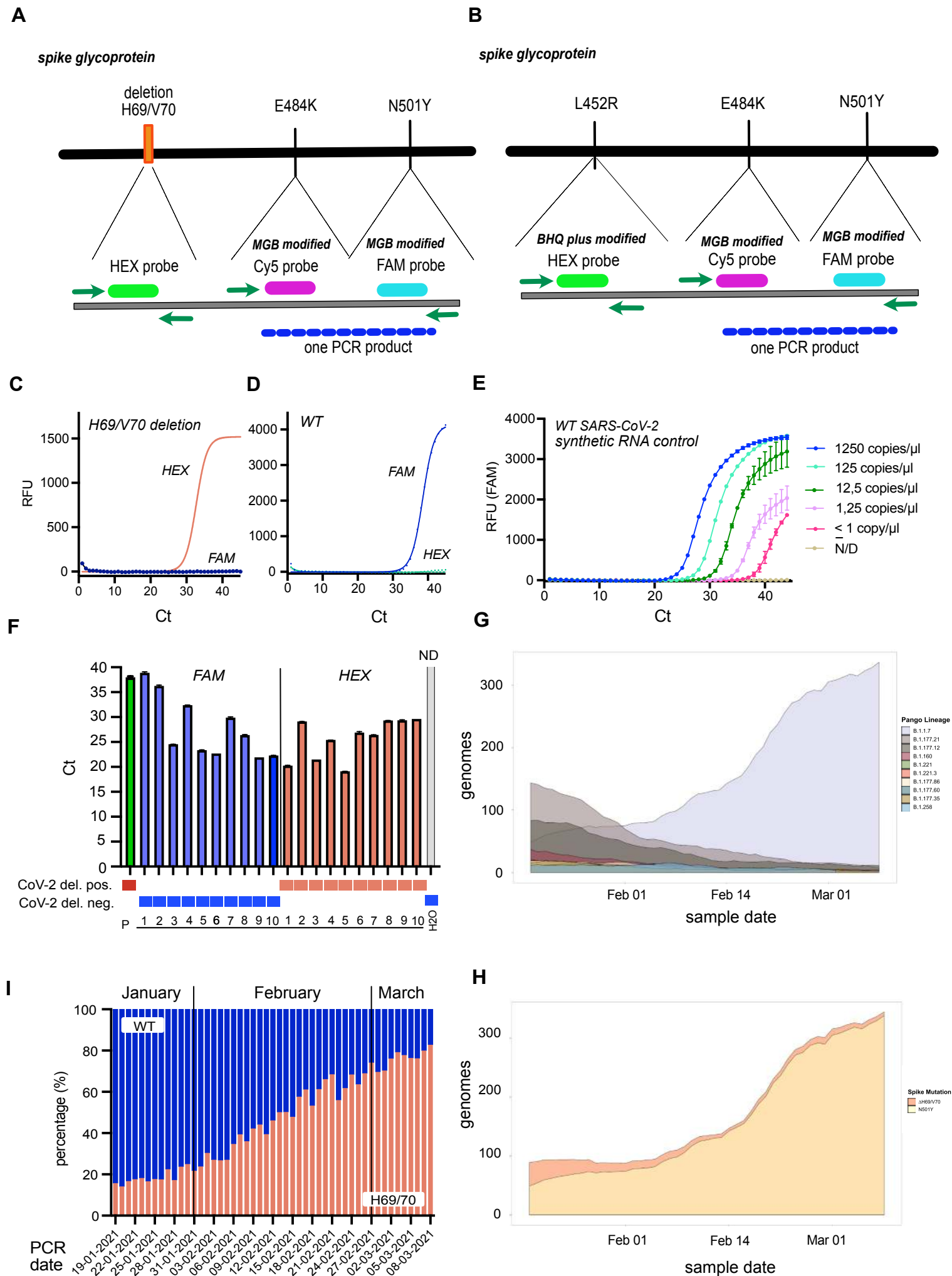


### Figure 3

All rights reserved. No reuse allowed without permission.

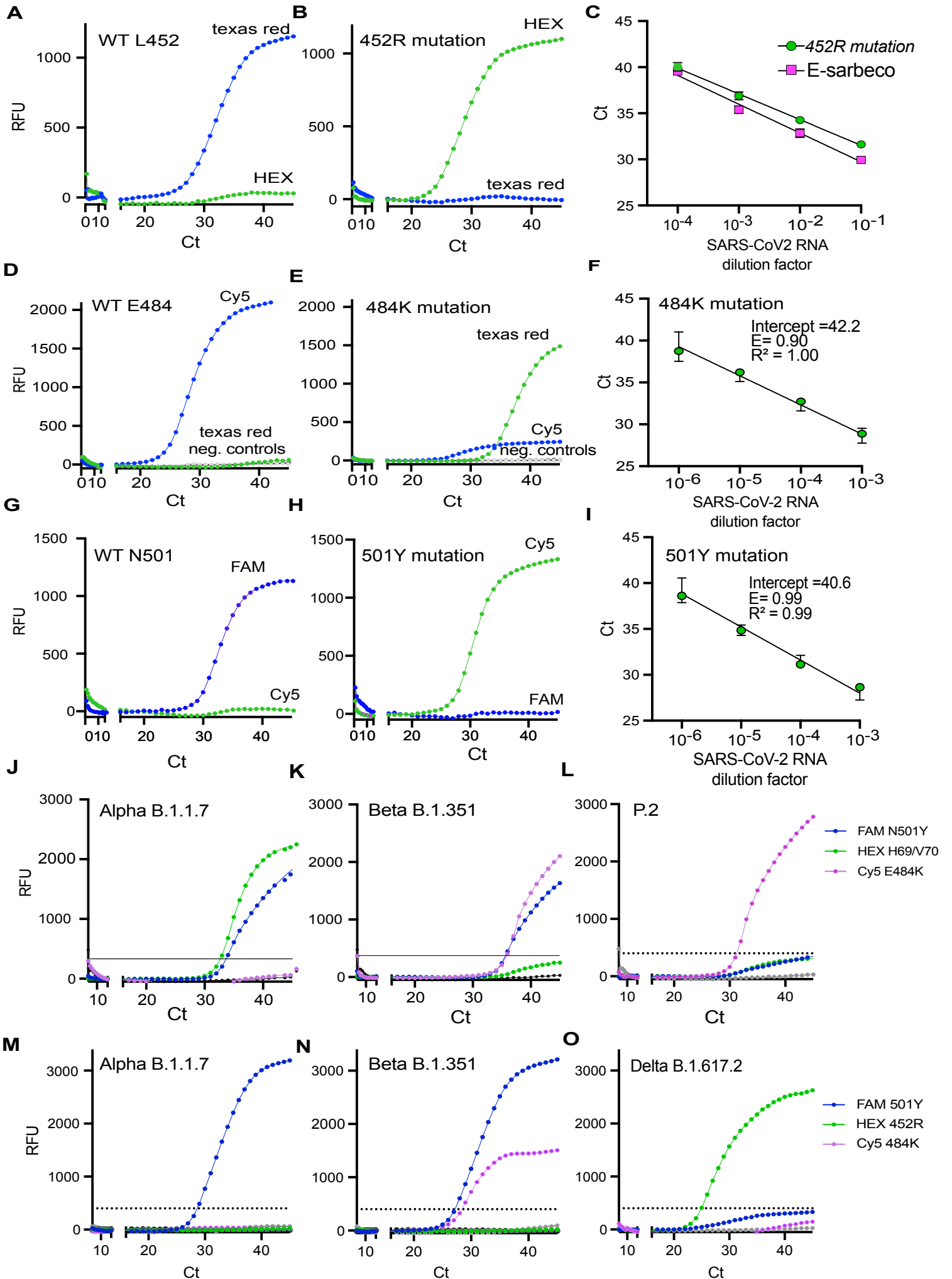


## Figure 4

### Large scale screening - single and multiplexed RT-qPCRs

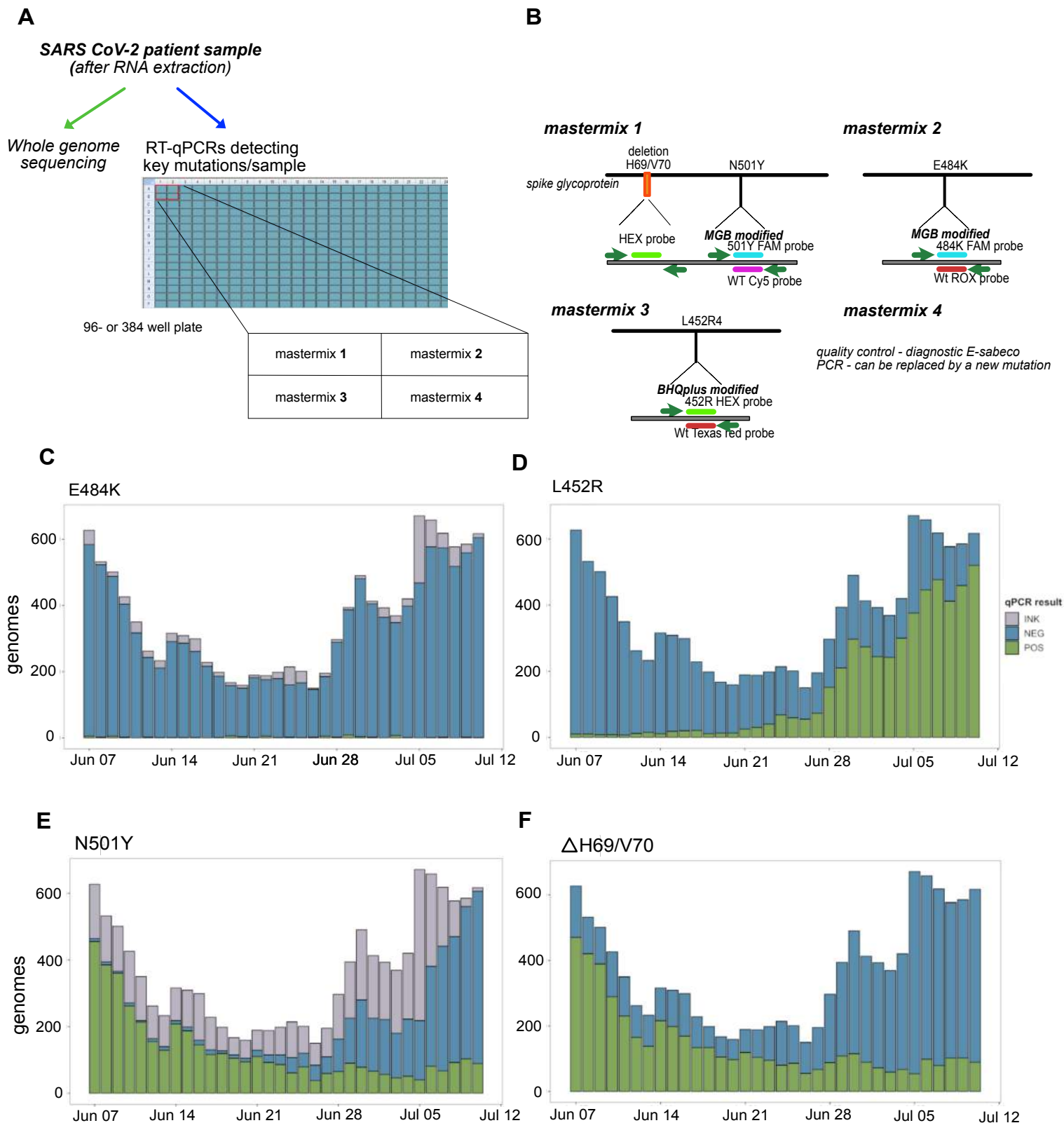
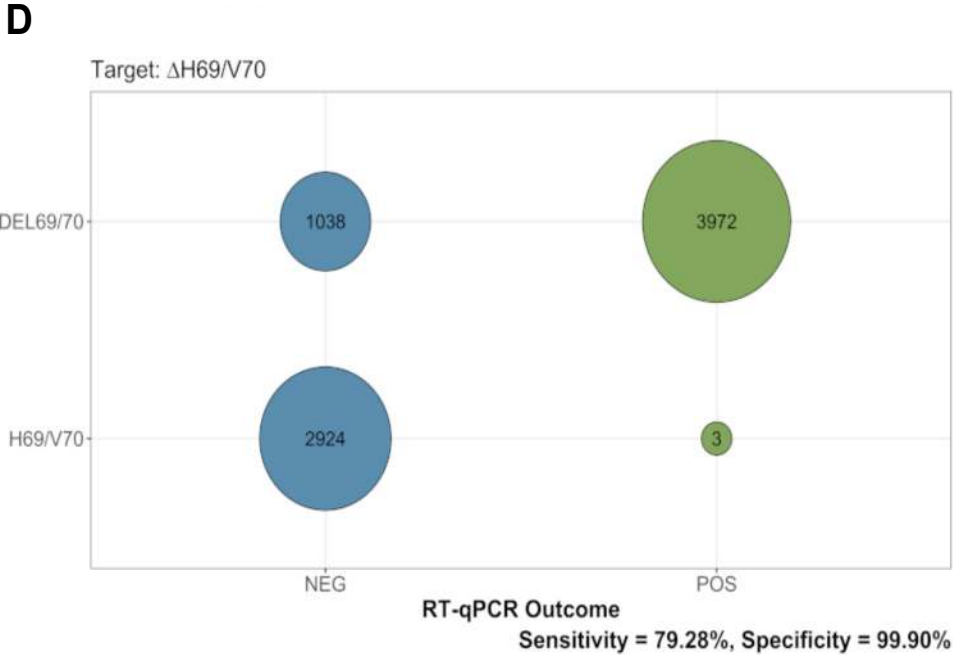
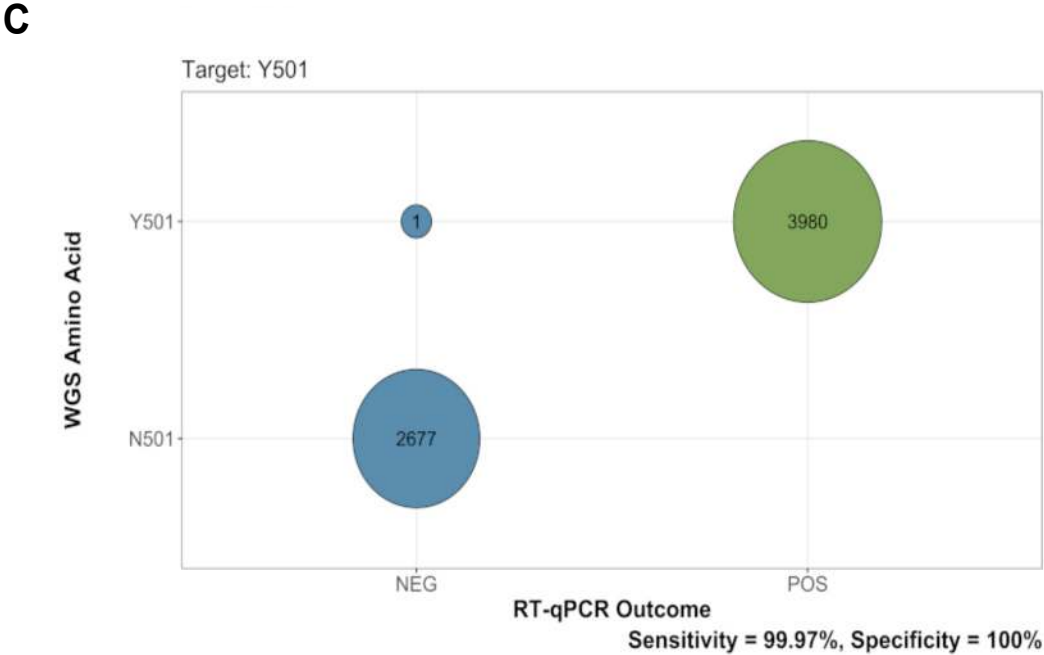
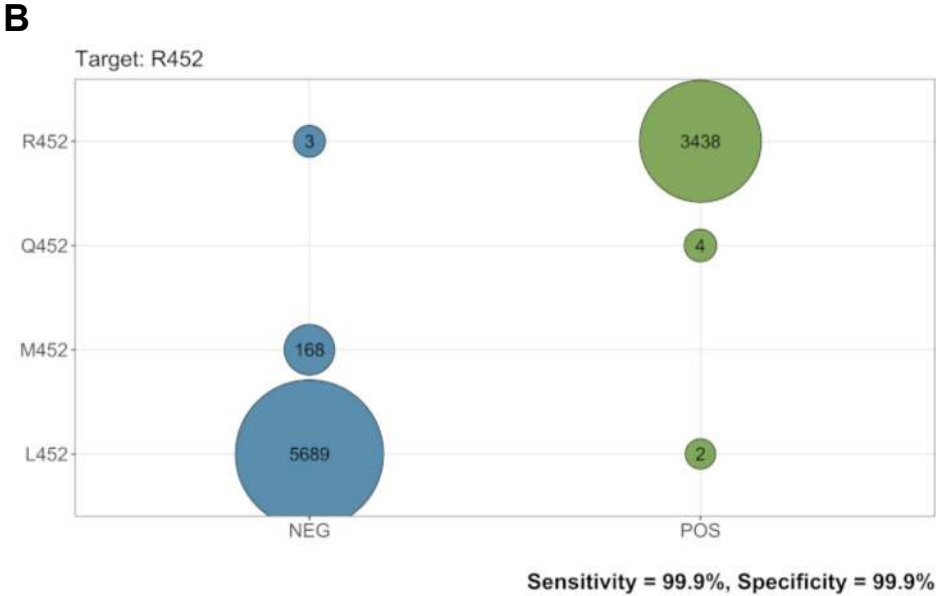
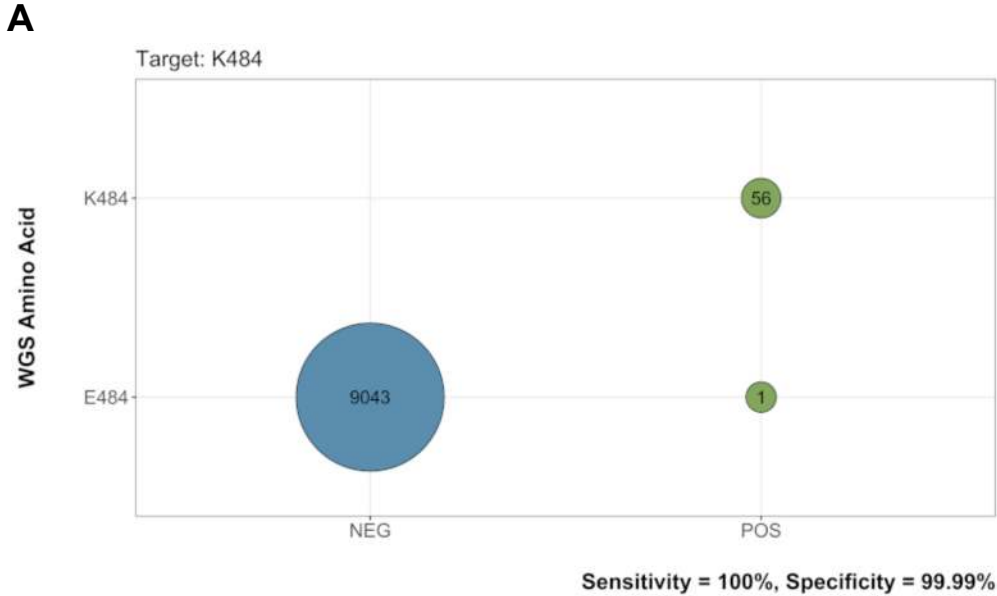
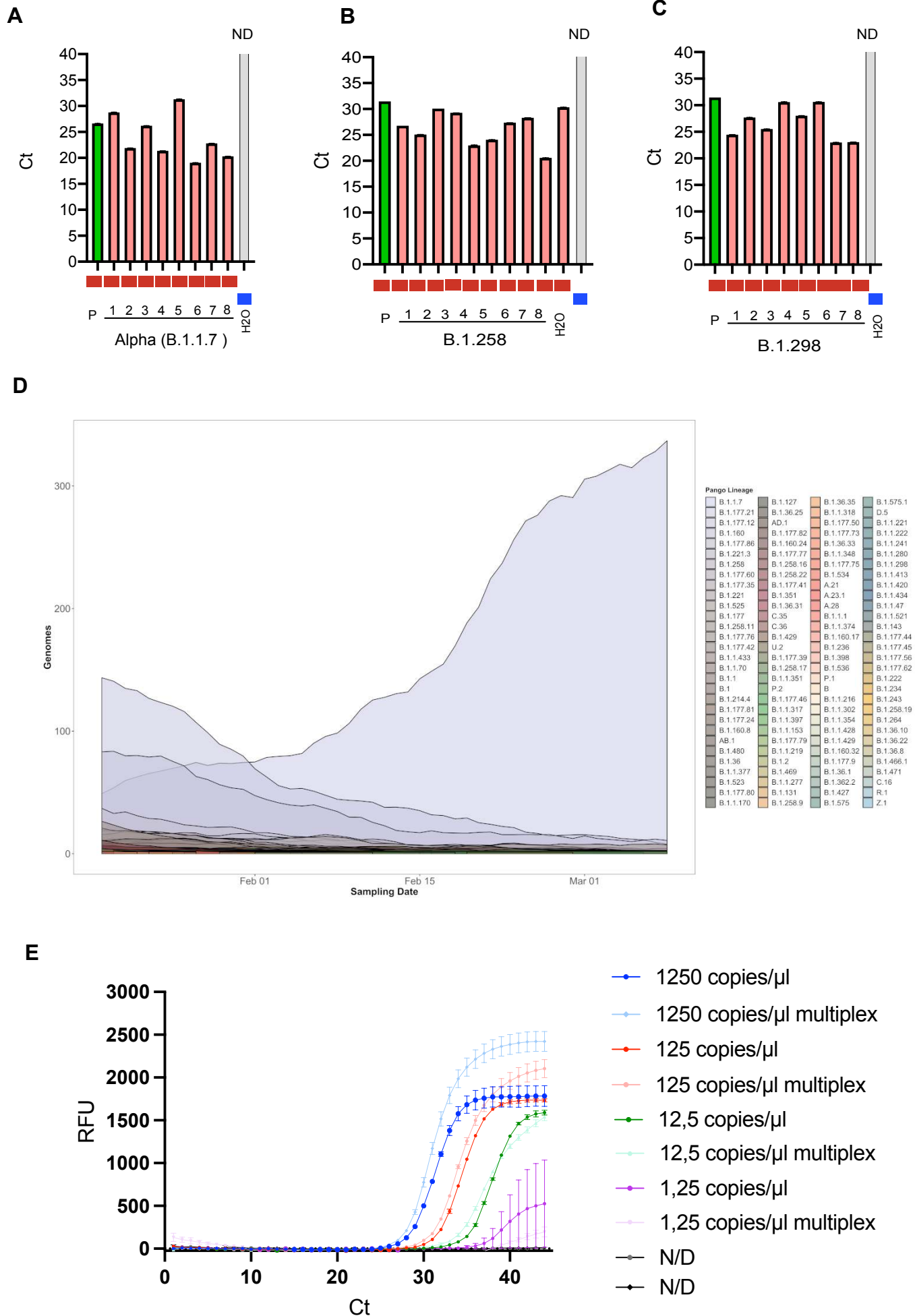




Figure 5

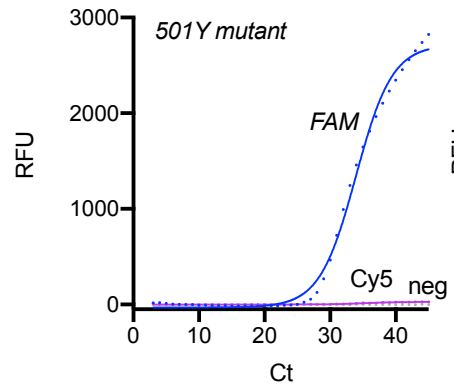


## Supplementary Fig.1

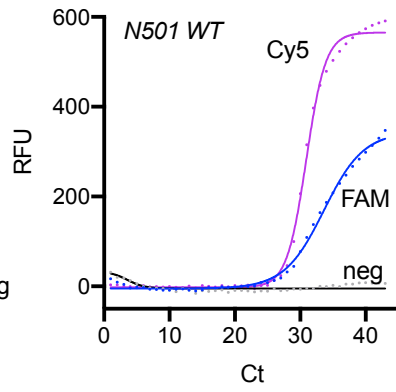


## Supplementary Fig.2

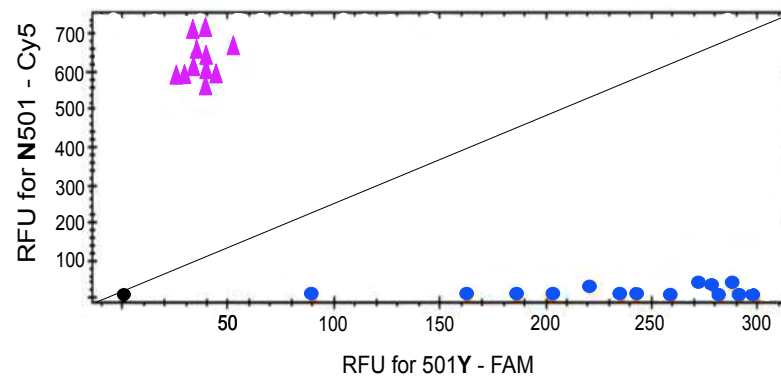
**A**



**B**



**C**



**G**

**D**

